





# The transcription factor ORA59 exhibits dual DNA binding specificity that differentially regulates ethylene- and jasmonic acid-induced genes in plant immunity

Young Nam Yang,<sup>1</sup> Youngsung Kim,<sup>1</sup> Hyeri Kim,<sup>1</sup> Su Jin Kim,<sup>1</sup> Kwang-Moon Cho,<sup>2</sup> Yerin Kim ,<sup>3</sup> Dong Sook Lee,<sup>1,†</sup> Myoung-Hoon Lee,<sup>1,§</sup> Soo Young Kim ,<sup>4</sup> Jong Chan Hong ,<sup>5</sup> Sun Jae Kwon,<sup>2</sup> Jungmin Choi,<sup>3</sup> and Ohkmae K. Park <sup>1,\*†</sup>

<sup>1</sup> Department of Life Sciences, Korea University, Seoul 02841, Korea

<sup>2</sup> Molecular Diagnosis Division, AccuGene, Incheon 22006, Korea

<sup>3</sup> Department of Biomedical Sciences, Korea University College of Medicine, Seoul 02841, Korea

<sup>4</sup> Department of Biotechnology and Kumho Life Science Laboratory, College of Agriculture and Life Sciences, Chonnam National University, Gwangju 61186, Korea

<sup>5</sup> Division of Life Science, Plant Molecular Biology and Biotechnology Research Center, Gyeongsang National University, Jinju 52828, Korea

\*Author for communication: omkim@korea.ac.kr

†Senior author

‡Present address: Animal and Plant Quarantine Agency, Foot and Mouth Disease Research Division, Gimcheon 39660, Korea

§Present address: Genuine Research, Seoul 06040, Korea

O.K.P. conceived and directed the project. Y.N.Y. and O.K.P. designed the research. Y.N.Y. performed most of the experiments. Y.K. performed protein purification and EMSA analysis. H.K. conducted ChIP-qPCR analysis. D.S.L. and M.H.L. participated in EMSA and ChIP-qPCR analysis. S.J.K. generated transgenic and VIGS lines. K.M.C., Y.K., S.J.K., and J.C. conducted RNA-seq analysis. S.Y.K. and J.C.H. participated in Y1H screening experiments. Y.N.Y. and O.K.P. analyzed the data and wrote the manuscript. All authors contributed to the review and editing of the manuscript.

The author responsible for distribution of materials integral to the findings presented in this article in accordance with the policy described in the Instructions for Authors (<https://academic.oup.com/plphys/pages/General-Instructions>) is Ohkmae Park (omkim@korea.ac.kr).

## Abstract

Jasmonic acid (JA) and ethylene (ET) signaling modulate plant defense against necrotrophic pathogens in a synergistic and interdependent manner, while JA and ET also have independent roles in certain processes, e.g. in responses to wounding and flooding, respectively. These hormone pathways lead to transcriptional reprogramming, which is a major part of plant immunity and requires the roles of transcription factors. ET response factors are responsible for the transcriptional regulation of JA/ET-responsive defense genes, of which ORA59 functions as a key regulator of this process and has been implicated in the JA-ET crosstalk. We previously demonstrated that *Arabidopsis thaliana* *GDSL LIPASE 1* (*GLIP1*) depends on ET for gene expression and pathogen resistance. Here, promoter analysis of *GLIP1* revealed ERELEE4 as the critical cis-element for ET-responsive *GLIP1* expression. In a yeast one-hybrid screening, ORA59 was isolated as a specific transcription factor that binds to the ERELEE4 element, in addition to the well-characterized GCC box. We found that ORA59 regulates JA/ET-responsive genes through direct binding to these elements in gene promoters. Notably, ORA59 exhibited a differential preference for GCC box and ERELEE4, depending on whether ORA59 activation is achieved by JA and ET, respectively. JA and ET induced ORA59 phosphorylation, which was required for both activity and specificity of ORA59. Furthermore, RNA-seq and virus-induced gene silencing analyses led to the identification of ORA59 target genes of distinct

functional categories in JA and ET pathways. Our results provide insights into how ORA59 can generate specific patterns of gene expression dynamics through JA and ET hormone pathways.

## Introduction

In nature, plants encounter a wide range of microbial pathogens with varying lifestyles and infection strategies. Upon pathogen recognition, plants rapidly activate defense responses, and the levels of resistance are influenced by hormone actions (De Vos et al., 2005; Pieterse et al., 2009). Salicylic acid (SA), jasmonic acid (JA), and ethylene (ET) are primary defense hormones that trigger immune signaling mechanisms (Dong, 1998; Pieterse et al., 2012). In the classic view, SA signaling enhances resistance against biotrophic and hemibiotrophic pathogens such as *Hyaloperonospora arabidopsidis* and *Pseudomonas syringae*, whereas JA and ET signaling activate resistance against necrotrophic pathogens such as *Alternaria brassicicola* and *Botrytis cinerea* (Feys and Parker, 2000; Glazebrook, 2005). Antagonism between SA and JA/ET and synergism between JA and ET have been mostly observed in studies of plant immunity, but there is also evidence of positive interactions between them (Penninckx et al., 1998; Thomma et al., 1998; Koornneef and Pieterse, 2008; Kim et al., 2013). These hormone signaling pathways are interconnected in a complex network and this signaling crosstalk enables plants to tailor defense responses efficiently (Kunkel and Brooks, 2002; Bostock, 2005; Spoel and Dong, 2008).

JA and ET modulate diverse developmental processes and defense responses in plants (Joo and Kim, 2007; Broekgaarden et al., 2015; Zhu and Lee, 2015). Their signaling pathways work by derepression mechanisms. MYC2/3/4 transcription factors play essential roles in JA signaling, and in the absence of JA, remain in repressed states by binding to transcriptional repressors JASMONATE ZIM-DOMAIN (JAZ) proteins (Chini et al., 2007; Thines et al., 2007). JA promotes the interaction between JAZs and the F-box protein CORONATINE INSENSITIVE 1 (COI1), resulting in degradation of JAZs and derepression of MYCs (Katsir et al., 2008; Yan et al., 2009; Sheard et al., 2010). The activated MYCs then regulate gene expression and various JA responses (Cheng et al., 2011; Fernandez-Calvo et al., 2011; Niu et al., 2011). ET INSENSITIVE 2 (EIN2), EIN3, and EIN3-LIKE 1 (EIL1) are key positive regulators of ET signaling (Chao et al., 1997; Alonso et al., 1999). In the absence of ET, ET receptors activate the Raf-like serine/threonine kinase CONSTITUTIVE TRIPLE RESPONSE 1 (CTR1), which phosphorylates EIN2 to repress its activity (Kieber et al., 1993). EIN3 and EIL1 are also targeted for degradation by EIN3-BINDING F-BOX PROTEIN 1 (EBF1) and EBF2 (Guo and Ecker, 2003; Potuschak et al., 2003). ET binding to ET receptors deactivates CTR1, which is followed by derepression of EIN2 (Chao et al., 1997). In the activation process, EIN2 is cleaved and its C-terminal fragment represses translation of EBF1/2

mRNA in the cytosol or translocates into the nucleus to stabilize EIN3/EIL1 (Ju et al., 2012; Qiao et al., 2012; Wen et al., 2012; Li et al., 2015). EIN3/EIL1 further activates downstream genes, including the ET RESPONSE FACTOR (ERF) family transcription factors (Solano et al., 1998; Chang et al., 2013). EIN3/EIL1 and ERFs regulate ET-mediated gene expression.

Plant defense against necrotrophic pathogens requires JA and ET, and synergistic and interdependent interactions between JA and ET have been described (Thomma et al., 1998; Koornneef and Pieterse, 2008). ERFs are important regulators of the JA-ET crosstalk, and in particular, ERF1 and OCTADECANOID-RESPONSIVE ARABIDOPSIS 59 (ORA59), belonging to the group IX ERF family, have been suggested to act as integrators of ET and JA signaling (Lorenzo et al., 2003; Pre et al., 2008). The expression of PATHOGENESIS-RELATED (PR) genes such as PLANT DEFENSIN 1.2 (PDF1.2) and BASIC CHITINASE (B-CHI) was synergistically induced by JA and ET, and abolished in JA-insensitive *coi1* and ET-insensitive *ein2* mutants, while depending on ERF1 and ORA59 (Penninckx et al., 1998; Lorenzo et al., 2003; Pre et al., 2008). Analysis of the PDF1.2 promoter indicated that ERF1 and ORA59 induce PDF1.2 expression through direct binding to GCC boxes in the PDF1.2 promoter (Zarei et al., 2011). Like other PR genes, the expression of ERF1 and ORA59 themselves exhibited a synergistic response to JA and ET, and was impaired in *coi1* and *ein2* mutants. The role of ERF1 and ORA59 in defense has been revealed in ERF1- and ORA59-overexpressing plants displaying enhanced resistance to necrotrophic pathogens (Berrocal-Lobo et al., 2002; Pre et al., 2008).

ERF1 and ORA59 have been determined to be regulated by EIN3 and their JA- and ET-responsive expression was abolished in *ein3 eil1* mutant (Solano et al., 1998; Zhu et al., 2011; Zander et al., 2012). Given that EIN3 is a positive regulator of ERF1 and ORA59, it was assessed whether EIN3 and EIL1 control JA and ET synergy on defense gene expression. JAZ proteins recruited HISTONE DEACETYLASE 6 (HDA6) as a corepressor to deacetylate histones and interacted with EIN3/EIL1 to repress EIN3/EIL1-mediated transcription (Zhu et al., 2011). JA led to JAZ degradation and removed JAZ-HDA6 from EIN3/EIL1, and ET enhanced EIN3/EIL1 accumulation, enabling EIN3/EIL1 to converge JA and ET signaling. The Mediator complex has been implicated in the regulation of diverse signaling pathways, connecting transcription factors with the RNA polymerase II machinery (Bäckström et al., 2007). The Mediator subunit MED25 physically interacted with several transcription factors, including ERF1, ORA59, and EIN3/EIL1, and was required for ERF1- and ORA59-activated PDF1.2 expression (Çevik et al., 2012; Yang et al., 2014). Meanwhile, SA suppressed JA-dependent

transcription by negatively affecting ORA59 protein abundance, suggesting that ORA59 acts as a node for SA and JA antagonism (Van der Does et al., 2013; He et al., 2017).

In this study, we report that the previously undefined cis-element ERELEE4 is critical for JA/ET-induced transcription and is frequently present in the promoters of JA/ET-responsive genes. In a yeast one-hybrid (Y1H) screening, ORA59 was identified as a specific transcription factor that binds to the ERELEE4 element, although ORA59 was previously known to regulate gene transcription by binding to GCC box. Depending on whether plants are exposed to JA or the ET precursor 1-aminocyclopropane-1-carboxylic acid (ACC) and ET, ORA59 exhibited preferential binding to GCC box and ERELEE4, respectively. The present study explores how two defense hormones JA and ET differentially regulate ORA59 and ORA59-responsive gene expression required for plant immunity.

## Results

### ERE is the cis-acting element for ET-responsive *GLIP1* expression

We previously demonstrated that Arabidopsis (*Arabidopsis thaliana*) *GDSL LIPASE 1* (*GLIP1*) is an ET-responsive defense gene that confers resistance to necrotrophic pathogens (Oh et al., 2005; Kwon et al., 2009; Kim et al., 2013, 2014). In an expression analysis, Col-0 plants exhibited strong *GLIP1* expression in response to ACC and ET, but a slight increase in *GLIP1* expression upon methyl JA (MeJA) treatment (Supplemental Figure S1, A and B), which is in line with previous results (Oh et al., 2005; Kim et al., 2013). However, both ACC- and MeJA-induced *GLIP1* expression was abolished in ET-insensitive *ein2* and *ein3 eil1* and JA-insensitive *coi1* mutants, indicating that *GLIP1* induction requires both ET and JA signaling pathways (Supplemental Figure S1, C and D). Whereas EIN2- and EIN3/EIL1-dependent *GLIP1* expression is consistent with our previous observation (Kim et al., 2013), COI1 dependency may result from EIN3 regulation by COI1-JAZ (Zhu et al., 2011).

To investigate how *GLIP1* expression is modulated by ET, the *GLIP1* promoter was searched for the cis-element critical for ET-responsive *GLIP1* expression. In previous studies, promoter analysis of ET- and JA-responsive *PR* genes led to the identification of the conserved sequence AGCCGCC or GCC box that serves as a binding site for ERFs (Ohme-Takagi and Shinshi, 1995; Hao et al., 1998; Brown et al., 2003). Accordingly, we expected the presence of GCC box in the *GLIP1* promoter and scanned the 2,966-bp *GLIP1* promoter region upstream of the transcription start site for cis-acting elements, using the PLACE program (<http://www.dna.affrc.go.jp/PLACE/>). This analysis revealed that the *GLIP1* promoter has no GCC box sequences and is enriched with binding motifs related to hormone and pathogen responses, which include two ET-responsive elements, ERELEE4 (AWTTCAAA) and RAV1AAT (CAACA) (Supplemental Table S1). ERELEE4 has been identified in promoter regions of tomato (*Lycopersicon esculentum*) *E4* and carnation

*GLUTATHIONE-S-TRANSFERASE 1* (*GST1*) genes, but poorly characterized (Montgomery et al., 1993; Itzhaki et al., 1994). RAV1AAT has been isolated as the binding motif for the Arabidopsis RELATED TO ABI3/VP1 1 (RAV1) transcription factor belonging to the APETALA2/ERF superfamily (Kagaya et al., 1999). ERELEE4 was located at 4 positions and RAV1AAT at 11 positions, here designated as ERE1–ERE4 and RAV1–RAV11, respectively, upward from the transcription start site. In the case of EREs, there were two different sequences, ATTTCAAA at ERE1, ERE3, and ERE4, and AATTCAAA at ERE2.

To examine whether ERE and RAV are key regulatory elements for ET-induced *GLIP1* expression, we introduced the chimeric constructs of the *GLIP1* promoter (*pGLIP1*) and the  $\beta$ -*GLUCURONIDASE* (*GUS*) reporter gene into Arabidopsis protoplasts and performed transient *GUS* reporter assays. In accordance with previous results (Kim et al., 2013), *pGLIP1* elevated *GUS* activity in response to ET and ACC, compared to mock treatments (Figure 1A; Supplemental Figure S2A). *pGLIP1* constructs with a series of 5'-deletions (*pGLIP1*-2466, -1466, -966, and -566) were made and assayed for their ability to drive ET- and ACC-induced *GUS* expression. As *pGLIP1* became shorter and RAV and ERE elements were lost, *GUS* activity decreased proportionally. No *GUS* activity was driven by *pGLIP1*-966 containing 3 RAV elements (RAV1–RAV3). The ability of ERE and RAV to respond to ET and ACC was further tested using synthetic promoters, in which a minimal promoter (TATA-box) was fused to four tandem copies (4x) of ERE and RAV and their mutated versions mERE and mRAV (Figure 1B; Supplemental Figure S2B). Among two ERE sequences in *pGLIP1*, more frequent ATTTCAAA was used for the synthetic promoter. The 4xERE promoter strongly triggered ET- and ACC-induced *GUS* expression compared to 4xRAV, suggesting that ERE is critical for ET- and ACC-mediated *GLIP1* expression. Their mutated versions had little effect on *GUS* expression. Next, *pGLIP1*-mediated *GUS* activity was measured after mutation of each ERE or four EREs at once (Figure 1C). *pGLIP1* with individual ERE mutations displayed significantly decreased *GUS* activity (47%–69% reduction) compared to the native promoter. *GUS* activity driven by *pGLIP1*<sup>mERE</sup>s with all four EREs mutated was largely eliminated. *pGLIP1* activity was further assessed in Col-0 plants harboring *pGLIP1*:*GUS* or *pGLIP1*<sup>mERE</sup>s:*GUS* reporters. Histochemical staining developed strong *GUS* signals in *pGLIP1*:*GUS* plants upon ACC treatment and in response to *B. cinerea* infection, which were largely abolished in *pGLIP1*<sup>mERE</sup>s:*GUS* plants (Supplemental Figure S3A). These results together demonstrate that ERE plays a major role in ET-responsive *GLIP1* expression.

The requirement of ERE elements for *GLIP1* expression was additionally assessed by generating transgenic plants, *pGLIP1*:*GLIP1*-GFP and *pGLIP1*<sup>mERE</sup>s:*GLIP1*-GFP, which expresses *GLIP1* fused to GREEN FLUORESCENT PROTEIN (GFP) at the C-terminus under the control of *pGLIP1* and *pGLIP1*<sup>mERE</sup>s, respectively, in the *glip1* mutant background. First, plants were infected with *A. brassicicola* and examined

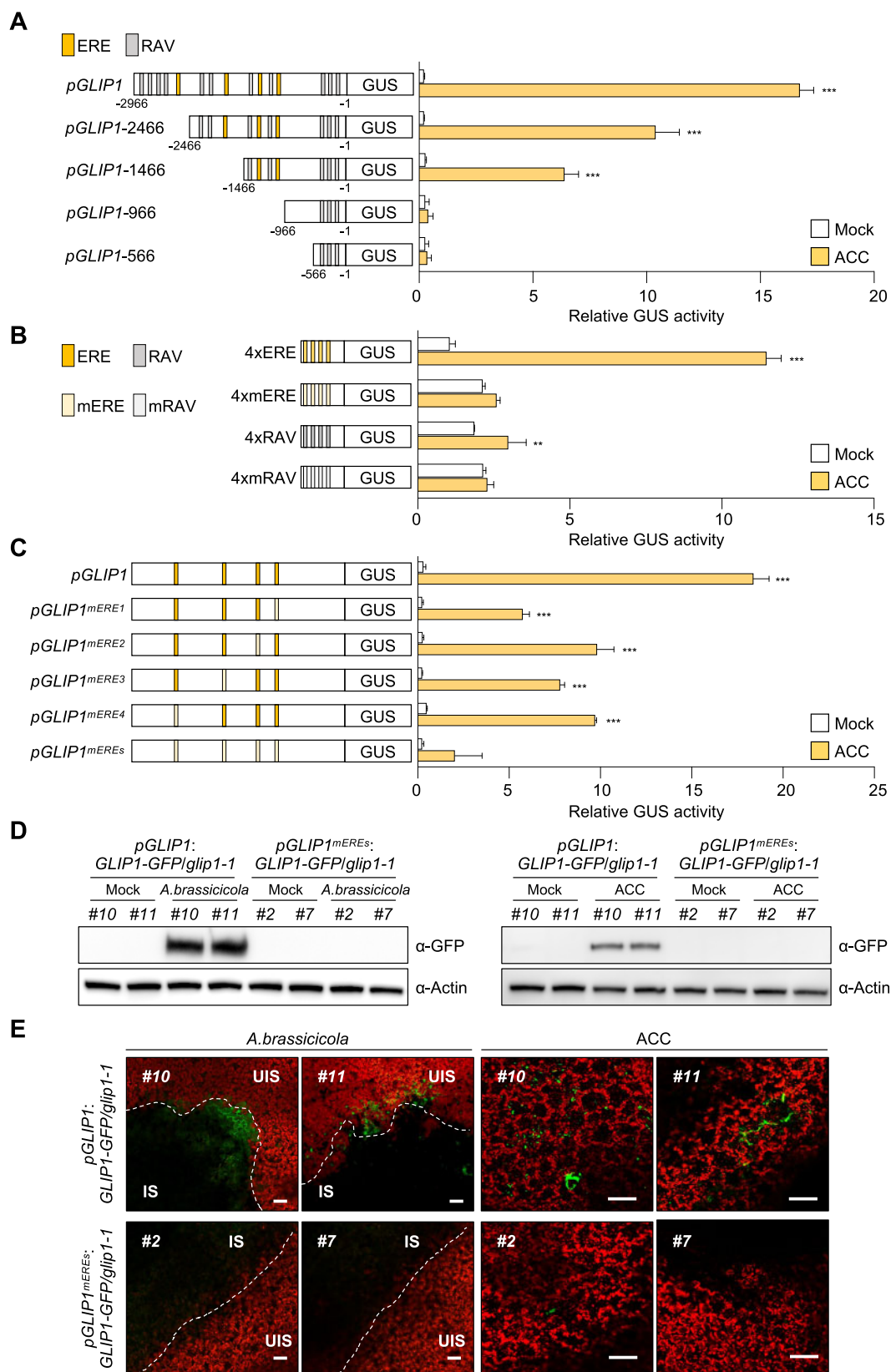


**Figure 1** ERE is the essential regulatory element in the *GLIP1* promoter. A, GUS reporter assays showing ACC-induced expression of the GUS reporter gene driven by the full-length and truncated *GLIP1* promoters. The left part illustrates deletions of the *GLIP1* promoter. The ERE and RAV elements in the *GLIP1* promoter are boxed in yellow and gray, respectively. B, GUS reporter assays showing ACC-induced expression of the GUS reporter gene driven by synthetic promoters of 4xERE and 4xRAV, and their mutant versions 4xmERE and 4xmRAV. The left illustrates synthetic promoters. C, GUS reporter assays showing ACC-induced expression of the GUS reporter gene driven by the *GLIP1* promoters with individual or all ERE mutations. The left illustrates ERE mutations of the *GLIP1* promoter. D, Immunoblot analysis of *GLIP1*-GFP expression in *A. brassicicola*-

for disease development. Unlike *pGLIP1<sup>mEREs</sup>:GLIP1-GFP*, *pGLIP1:GLIP1-GFP* expression restored disease resistance in *glip1* (Supplemental Figure S3, B–D). Consistently, *GLIP1-GFP* transcripts and *GLIP1-GFP* proteins accumulated and GFP fluorescence was detected in *pGLIP1:GLIP1-GFP* plants, but not in *pGLIP1<sup>mEREs</sup>:GLIP1-GFP* plants, in response to *A. brassicicola* and ACC treatments (Figure 1, D and E; Supplemental Figure S3E). These results together indicate that ERE elements are essential for *GLIP1* expression during the immune response.

### ORA59 is an ERE-binding transcription factor

Next, we searched for a transcription factor(s) that regulate ET-responsive *GLIP1* expression, and for this, performed Y1H screening using the ERE sequence ATTTCAAA as bait. The yeast strain, harboring three tandem copies of ERE fused to *HIS3* and *lacZ* genes, was transformed with a prey library composed of 1050 Arabidopsis transcription factor cDNAs (Welchen et al., 2009). Screening of  $2 \times 10^6$  transformants yielded 84 positive clones growing on selective media lacking histidine and containing 3-amino-1,2,4-triazole (3-AT) (Supplemental Table S2). Among these positive clones, ORA59, RELATED TO AP2.2 (RAP2.2), and CAPRICE-LIKE MYB3 (CPL3) were subjected to further analysis, as they most strongly increased  $\beta$ -galactosidase reporter activity. Retransformation with the recovered plasmid DNAs enabled yeast cells to grow on selective media (Figure 2A).

To test for *in vitro* binding of ORA59, RAP2.2, and CPL3 to the ERE element, we performed an electrophoretic mobility shift assay (EMSA) using recombinant proteins purified from *Escherichia coli* and DNA probes of two ERE sequences ATTTCAAA and AATTCAAA (Figure 2B; Supplemental Figure S4A). Whereas ORA59 formed a shifted band, RAP2.2 and CPL3 exhibited weak binding. ORA59 had similar levels of binding activity to these two ERE sequences. The addition of excess amounts of unlabeled ERE probes effectively competed the binding, verifying specific ORA59 binding to the ERE sequences (Figure 2C). Transient GUS reporter assays were then performed to determine whether they can induce transcription through ERE *in vivo* (Figure 2D). The *pGLIP1* and synthetic 4xERE and 4xRAV promoters, and their mutant versions *pGLIP1<sup>mEREs</sup>*, 4xmERE, and 4xmRAV were used as reporter constructs, and together with effector constructs of CPL3, RAP2.2, and ORA59, were transformed into Arabidopsis protoplasts. Whereas ORA59 strongly activated *pGLIP1*- and 4xERE-mediated GUS expression, slight GUS expression driven by both *pGLIP1* and *pGLIP1<sup>mEREs</sup>* was observed with RAP2.2, and no GUS activity was observed with

CPL3. Transactivation by ORA59 was dependent on ERE in reporter genes, because no activity was detected for reporters with *pGLIP1<sup>mEREs</sup>* and 4xmERE or with 4xRAV and 4xmRAV. These results suggest that ORA59 controls *GLIP1* expression via ERE binding. Like ORA59, ERF1 functions in ET and JA signaling pathways (Lorenzo et al., 2003; Pre et al., 2008), and therefore, it was tested whether ERF1 also has binding activity to the ERE element. In the EMSA analysis, ERF1 recombinant proteins bound to both ERE sequences (Supplemental Figure S5).

Because GCC box has been determined as a specific binding site for ORA59 and other ERFs in previous reports (Ohme-Takagi and Shinshi, 1995; Hao et al., 1998; Zarei et al., 2011), the binding activity of ORA59 to GCC box and ERE was compared using recombinant ORA59 proteins. In addition to full-length ORA59, several truncated forms of ORA59 were prepared (Supplemental Figure S4, B and C). In the EMSA analysis, full-length ORA59 bound to GCC box more strongly than to ERE (Figure 2, E and F). Noticeably, N-terminal deletion (F1) dramatically enhanced ORA59 binding to GCC box, but rather abrogated ERE-binding activity. In contrast, ORA59 with partial C-terminal deletion (F3) showed much stronger ERE binding. We failed to secure soluble ORA59 proteins with deletion of the entire C-terminal region after the AP2 domain. The C-terminal (F2) and N-terminal (F4) portions alone exhibited no DNA binding activities, as expected for ORA59 without the DNA-binding AP2 domain. AP2 domain alone had stronger binding activity to ERE than to GCC box, which was reversed for full-length ORA59. These results suggest that ORA59 may form distinct structural conformations in binding to ERE and GCC box, and the N-terminal and C-terminal portions of ORA59 affect ORA59 binding to ERE and GCC box in different manners. The N-terminal portion may have a positive or negative effect on ORA59 binding to ERE and GCC box, respectively, and this may be the opposite for the C-terminal portion.

### ORA59 binding to ERE and GCC box is differentially regulated in ET and JA signaling

To study how ORA59 interacts with ERE and GCC box elements *in vivo*, we additionally prepared transgenic plants (35S:ORA59-GFP) overexpressing ORA59 fused to GFP at the C-terminus under the control of the CaMV 35S promoter (Supplemental Figure S6, A and B). As observed in a previous study (Pre et al., 2008), 35S:ORA59-GFP plants showed a dwarf phenotype. Basal transcript levels of *GLIP1* were increased in 35S:ORA59-GFP plants, and ACC- and *B. cinerea*-induced

#### Figure 1 Continued

and ACC-treated *pGLIP1:GLIP1-GFP glip1* and *pGLIP1<sup>mEREs</sup>:GLIP1-GFP glip1* plants. Protein extracts were subjected to immunoblotting with anti-GFP and anti-Actin antibodies. Actin levels served as a control. E, Confocal images of *GLIP1-GFP* expression in *A. brassicicola*- and ACC-treated *pGLIP1:GLIP1-GFP glip1* and *pGLIP1<sup>mEREs</sup>:GLIP1-GFP glip1* plants. Bars, 100  $\mu$ m. Two independent transgenic lines were used in all experiments. In (A–C), transfected protoplasts were treated with mock (water) and ACC (200  $\mu$ M) for 6 h. Values represent means  $\pm$ SD (standard deviation) ( $n = 3$  biological replicates). Asterisks indicate significant differences from mock treatment as determined by one-way ANOVA with Tukey test (\*\* $P < 0.01$ ; \*\*\* $P < 0.001$ ). In (D and E), 6-week-old plants were treated with ACC (1 mM) for 6 h or with 5  $\mu$ L droplets of *A. brassicicola* spore suspensions ( $5 \times 10^5$  spores mL<sup>-1</sup>) for 2 d. IS, infected site; UIS, uninfected site.

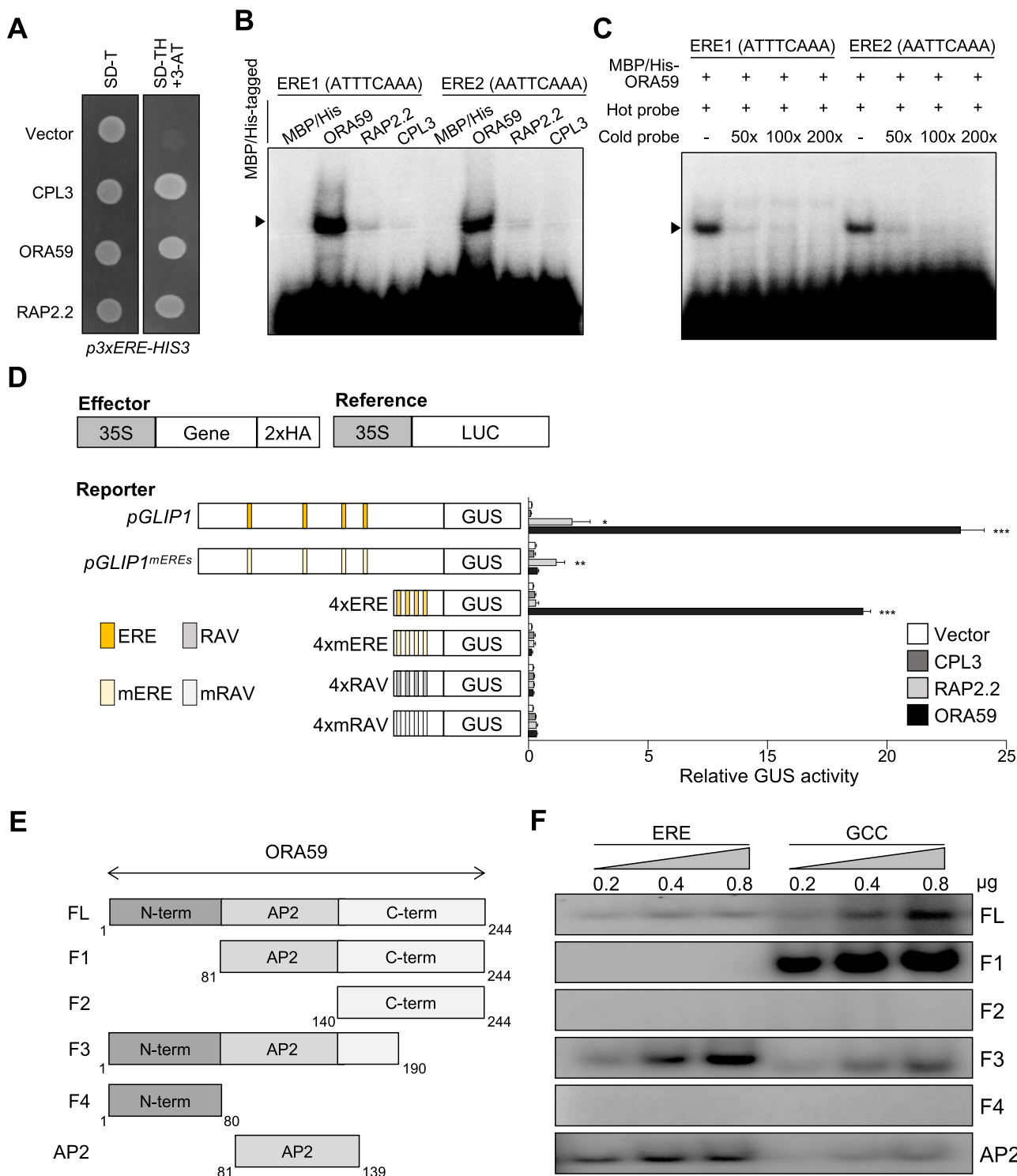


**Figure 2** ORA59 is the specific ERE-binding transcription factor. **A**, Isolation of ERE-binding transcription factors by Y1H screening. Yeast cells harboring the 3xERE-HIS3 reporter gene were transformed with effector constructs *CPL3*, *ORA59*, and *RAP2.2*. Transcription factor binding to ERE was tested on a selective medium lacking tryptophan and histidine, and supplemented with 0.2 mM 3-amino-1,2,4-triazole (SD-TH + 3-AT). **B**, DNA binding of *ORA59*, *RAP2.2*, and *CPL3* to the two ERE sequences ATTTCAAA (ERE1) and AATTCAAA (ERE2). Recombinant proteins were incubated with biotin-labeled ERE oligonucleotide probes in EMSA. **C**, Competition assays. *ORA59* binding to ERE1/2 was competed with increasing amounts (50×, 100×, 200×) of unlabeled oligonucleotide competitors. **D**, Transactivation analysis showing the *ORA59*-mediated *GUS* reporter gene induction driven by the *GLIP1* and 4xERE synthetic promoters. The left part illustrates reference, effector, and reporter constructs. Reporter DNAs, either alone or together with effector DNAs, were transfected into protoplasts, and *GUS* activity was measured. Luciferase (LUC) expressed under control of the CaMV 35S promoter was used as an internal control (reference). Values represent means ± SD ( $n = 3$  biological replicates). Asterisks indicate significant differences from vector control as determined by one-way ANOVA with Tukey test (\* $P < 0.05$ ; \*\* $P < 0.01$ ; \*\*\* $P < 0.001$ ). 35S, CaMV 35S; 2xHA, two copies of the HA tag sequence. **E**, Schematic diagram of full-length and truncated *ORA59* proteins prepared for EMSA. **F**, DNA binding of different forms of *ORA59* to the ERE and GCC box elements. Increasing amounts (0.2, 0.4, and 0.8 μg) of recombinant proteins were incubated with biotin-labeled ERE and GCC box oligonucleotide probes in EMSA. FL, full-length; GCC, GCC box.

*GLI1* expression was diminished in *ora59* mutant, confirming that ORA59 is the key regulator of *GLI1* expression (Supplemental Figure S6C). *35S:ORA59-GFP* plants exhibited enhanced resistance against *B. cinerea*, as determined by lesion size and abundance of fungal actin gene (Supplemental Figure S6D). In contrast, susceptibility to *B. cinerea* was increased in *ora59* plants. Among independent lines, *35S:ORA59-GFP* (#6) was used for further study.

ORA59-GFP protein levels were monitored in *35S:ORA59-GFP* plants exposed to ACC and MeJA. ORA59-GFP proteins rapidly disappeared in the presence of the protein synthesis inhibitor cycloheximide (CHX), which was repressed by treatment with the proteasome inhibitor MG132 (Figure 3A). ORA59-GFP protein abundance was elevated in ACC- or MeJA-treated *35S:ORA59-GFP* plants. These results indicate that ORA59 undergoes 26S proteasome-dependent degradation, and ET and JA enhance the stability of ORA59 proteins.

To examine ORA59 binding to ERE and GCC box *in planta*, nuclear extracts were prepared from ACC-, ET-, and MeJA-treated *35S:ORA59-GFP* plants and assessed for binding to these elements by EMSA. Noticeably, nuclear extracts from ACC-, ET-, and MeJA-treated *35S:ORA59-GFP* plants showed DNA-binding activities with differential preferences for ERE and GCC box, respectively, which were largely diminished in Col-0 and *ora59* extracts (Figure 3, B and C; Supplemental Figure S7). In the EMSA supershift analysis, ERE- and GCC box-bound proteins from *35S:ORA59-GFP* plants were supershifted by an anti-GFP antibody but not by pre-immune IgG (Supplemental Figure S8). These results imply that DNA–protein complexes observed are mostly of ORA59 expressed in *35S:ORA59-GFP* plants. Col-0 nuclear extracts, albeit weakly binding, retained the hormone-dependent preference for ERE and GCC box.

The Ser-rich sequence of ORA59 (Supplemental Figure S4B) led us to speculate that DNA binding properties of ORA59 may be regulated by posttranslational modifications, such as phosphorylation. To address this, nuclear extracts of *35S:ORA59-GFP* plants were immunoprecipitated with an anti-GFP antibody, and the isolated proteins were subjected to Western blotting with an anti-phospho-Ser/Thr antibody. It revealed that ORA59 is phosphorylated in ACC- and MeJA-treated plants (Figure 3B). To further verify this, *35S:ORA59-GFP* nuclear extracts were treated with lambda phosphatase before incubation with DNA probes. Phosphatase treatment led to dephosphorylation of ORA59, which was accompanied by a substantial reduction in ORA59 binding to ERE and GCC box, and particularly, lack of hormone-dependent binding sequence specificity (Figure 3D). When accumulated after MG132 treatment, ORA59-GFP proteins showed much lower level of phosphorylation and similar levels of reduced binding to ERE and GCC box without hormone-dependent preference, compared to those treated with ACC and MeJA (Figure 3E). This indicates that ORA59 is normally phosphorylated to a certain extent and the phosphorylation level is increased in response to ET and JA. These results suggest that

ET- and JA-mediated ORA59 phosphorylation is critical for ORA59 activity.

Considering the role of ORA59 in the ET-JA crosstalk, the next question was how ORA59 binds to ERE and GCC box when activated by two hormones simultaneously. To investigate this, *35S:ORA59-GFP* plants were co-treated with ACC and JA, and then subjected to EMSA. A combination of ACC and JA did not further increase DNA binding of ORA59, nor did it change ORA59 protein abundance, compared to treatment with each hormone (Figure 3F). In contrast, the level of ORA59 phosphorylation was largely increased by ACC and MeJA co-treatments. We then examined whether hormone-dependent DNA binding properties of ORA59 are associated with transcriptional activity. GUS reporter assays were conducted using 4xERE and 4xGCC box synthetic promoters. In Col-0 protoplasts, ACC treatment induced a large increase in transcription through ERE but a less increase through GCC box (Figure 3G). Conversely, a large increase was observed with GCC box but a modest increase with ERE in response to MeJA treatment. Simultaneous treatments with ACC and MeJA led to a synergistic increase in GUS activity through both ERE and GCC box. This transcriptional activation was not observed with mutated elements and significantly decreased in *ora59* protoplasts. These results suggest that ET- and JA-regulated transcription is associated with differential DNA binding of ORA59, and ORA59 regulates ET and JA synergy at the level of transcriptional activation, but not at the level of DNA binding.

### ORA59 regulates gene expression by direct binding to ERE and GCC box

It was then determined whether other genes are also regulated by ORA59 in ET/JA-dependent ways. We found that *PDF1.2* genes have different distributions of ERE and GCC box in their promoters such that promoters of *PDF1.2a*, *PDF1.2b*, and *PDF1.2c* have a single GCC box, one GCC box and two ERE, and a single ERE elements, respectively (Figure 4A). We conducted GUS reporter assays using *PDF1.2* promoters. Whereas GUS expression driven by *PDF1.2* promoters was induced by both ACC and MeJA, *PDF1.2a* with only GCC box and *PDF1.2c* with only ERE responded more strongly to MeJA and ACC, respectively, than to the other (Figure 4B). Likewise, mutations of respective elements in *PDF1.2* promoters largely affected transcriptional activation, and in particular, mutation of either ERE or GCC box in the *PDF1.2b* promoter containing both elements more significantly reduced ACC- or MeJA-induced transcription, respectively. Gene expression analysis in Col-0 plants showed that endogenous transcript levels of *PDF1.2* genes were increased by ACC and MeJA treatments with similar preference for hormones observed in GUS reporter assays, and this increase was abolished in *ora59* plants (Figure 4C).

Given that ORA59 binds to ERE and GCC box in EMSA, we performed chromatin immunoprecipitation (ChIP)-qPCR analysis to examine whether ERE- and GCC box-driven transcriptional activation is induced through direct ORA59

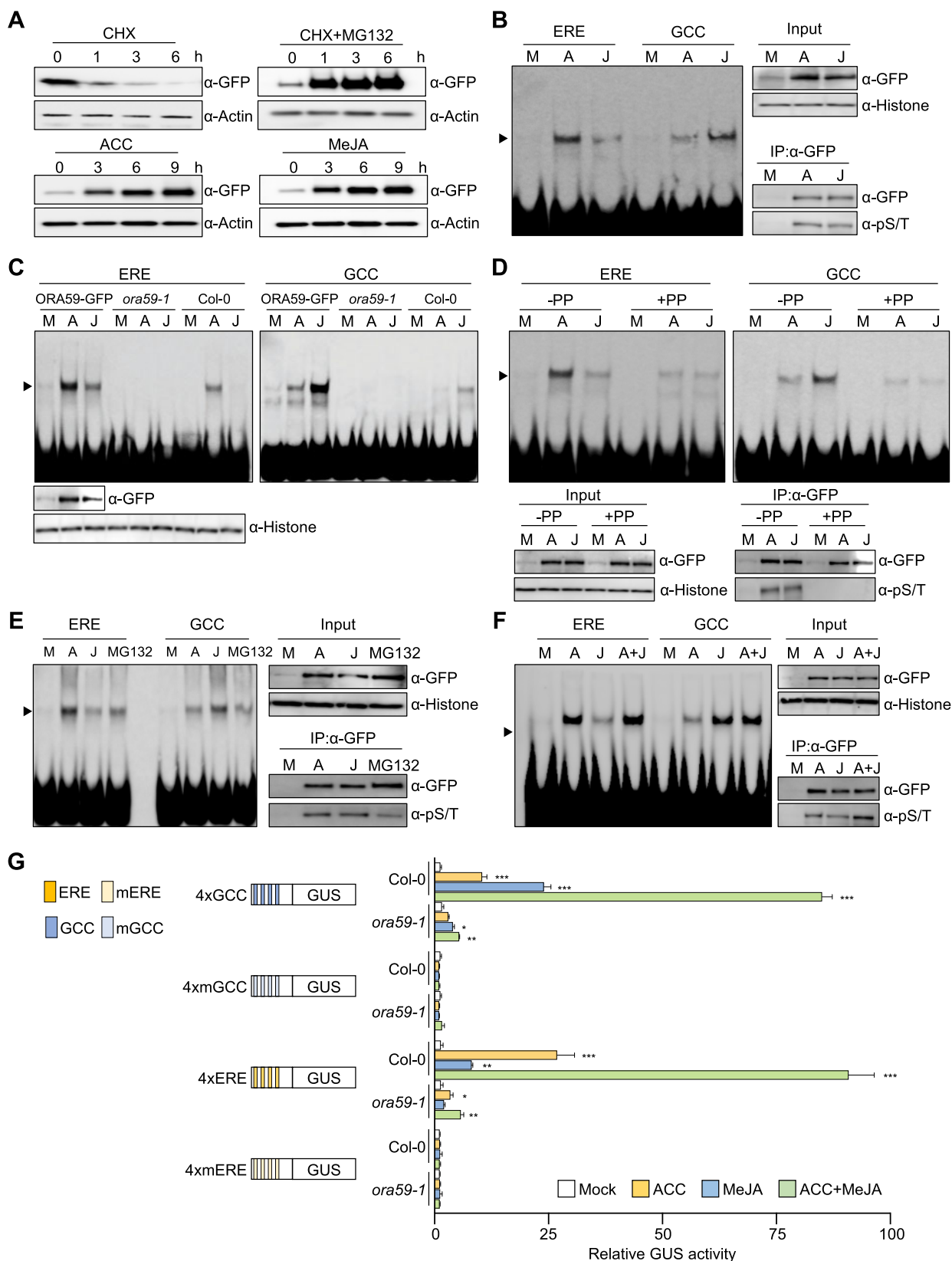


**Figure 3** ORA59 binding to ERE and GCC box is regulated in ACC- and JA-dependent manners. **A**, Immunoblot analysis of ORA59 stability in 35S:ORA59-GFP plants. Six-week-old plants were treated with cycloheximide (100  $\mu$ M), MG132 (50  $\mu$ M), ACC (1 mM), and MeJA (100  $\mu$ M) for the indicated times. Protein extracts were subjected to immunoblotting with anti-GFP and anti-Actin antibodies. Actin levels served as a control. **B**, EMSA analysis of nuclear extracts from 35S:ORA59-GFP plants. Six-week-old plants were treated with ACC (1 mM) and MeJA (100  $\mu$ M) for 6 h. Nuclear extracts were incubated with biotin-labeled ERE and GCC box oligonucleotide probes in EMSA. **C**, EMSA analysis of nuclear extracts from 35S:ORA59-GFP, *ora59-1*, and Col-0 plants. Six-week-old plants were treated with ACC (1 mM) and MeJA (100  $\mu$ M) for 6 h. Nuclear extracts were



binding to these elements in the *GLIP1* and *PDF1.2* promoters. 35S:ORA59-GFP plants were treated with ACC and MeJA, and their extracts were used for precipitating ORA59-bound DNA fragments with an anti-GFP antibody. In the *GLIP1* promoter, all four ERE-containing fragments were enriched in ORA59 binding, and this enrichment was increased more with ACC treatment than with MeJA (Figure 4, A and D). In addition, ORA59 binding was greatly enriched at ERE and GCC box sites of the *PDF1.2a*, *PDF1.2b*, and *PDF1.2c* promoters in response to ACC and MeJA treatments, respectively, which was consistent with the results of transcriptional activation (Figure 4E). No binding of ORA59 was observed in negative control fragments without ERE and GCC box sequences. These results indicate that ORA59 regulates ET- and JA-responsive gene expression by binding to ERE and GCC box directly and with hormone-dependent differential preference.

### Identification of ORA59-regulated ET- and JA-responsive genes by RNA-seq analysis

Based on differential responses of ORA59 to ACC and MeJA in gene regulation, we speculated that ORA59 may regulate distinct gene sets in the ET and JA pathways. Therefore, to identify ET- and JA-responsive ORA59 downstream genes, we performed RNA-sequencing (RNA-seq) analysis using biological replicates of ACC- and MeJA-treated Col-0 and *ora59* plants (Supplemental Table S3). Differentially expressed genes (DEGs) between mock (water) and ACC/MeJA treatments were selected in Col-0 and *ora59* plants based on the cutoff (adjusted *P* (*P*<sub>adj</sub>) < 0.05, log<sub>2</sub> fold change (|log<sub>2</sub> FC|) ≥ 1). Col-0 had far more DEGs than *ora59* mutant. 516 and 105 genes were differentially expressed in ACC-treated Col-0 and *ora59*, and 683 and 134 genes in MeJA-treated Col-0 and *ora59*, respectively (Figure 5A). This implies that ORA59 is an essential regulator of gene expression in ET and JA responses. Considering that DEGs in *ora59* mutant are ORA59-independent, among 516 and 683 DEGs in ACC- and MeJA-treated Col-0, after subtracting 37 and 87 genes co-regulated in Col-0 and *ora59*, 479 and 596 genes were defined as ACC- and MeJA-responsive ORA59-regulated genes,

respectively (Figure 5B). It was noted that the majority of ORA59-dependent genes were upregulated in response to ACC (346 out of 479, 72.2%) and in response to MeJA (443 out of 596, 74.3%), suggesting that ORA59 primarily functions as a transcriptional activator of gene expression. The overlap between ACC- and MeJA-responsive ORA59-regulated genes was relatively small, and only 54 genes were shared (Figure 5B).

We then performed Gene Ontology (GO) enrichment analysis of ORA59-regulated DEGs, using GO Biological Process (BP) terms provided by PANTHER database (<http://geneontology.org>) (Supplemental Table S4). The analysis revealed that ACC-responsive DEGs are enriched in responses to stress, oxygen-containing compounds, stimulus, and oxygen levels GO BP terms, while MeJA-responsive DEGs are enriched in metabolic processes of organic acids, S-glycosides, and secondary metabolites, and in responses to stress and chemicals GO BP terms (Figure 5C). Enriched GO BP terms indicate that ACC and MeJA regulate distinct BPs in an ORA59-dependent manner, only co-regulating the “response to stress.” We then determined the occurrence and enrichment of ERE and GCC box in promoters of ORA59-regulated ACC- and MeJA-responsive genes, compared to whole Arabidopsis 34362 genes. Noticeably, ERE was present at a much higher frequency (28.5%) than GCC box (4.4%) in whole gene promoters (Figure 5D). Statistically significant enrichment of ERE was observed in both ACC (Fisher’s exact test  $P = 3.38 \times 10^{-8}$ )- and MeJA (Fisher’s exact test  $P = 2.12 \times 10^{-8}$ )-responsive genes, but GCC box was only enriched in MeJA (Fisher’s exact test  $P = 3.98 \times 10^{-3}$ )-responsive genes.

### Identification of ORA59 target genes involved in disease resistance

For further functional analysis, we focused primarily on genes whose expression was increased by ACC and MeJA treatments. Among ACC- and MeJA-responsive DEGs, 63 (|log<sub>2</sub> FC| ≥ 2) and 55 (|log<sub>2</sub> FC| ≥ 3) upregulated genes were selected from the five most significantly enriched GO BP terms, respectively, and their expression was validated by

#### Figure 3 Continued

incubated with biotin-labeled ERE and GCC box oligonucleotide probes in EMSA. D, Effect of phosphatase treatment on DNA binding of ORA59. Six-week-old plants were treated with ACC (1 mM) and MeJA (100 μM) for 6 h. Nuclear extracts were treated with lambda phosphatase for 30 min before incubation with biotin-labeled ERE and GCC box oligonucleotide probes in EMSA. E, Effect of MG132 treatment on DNA binding of ORA59. Six-week-old plants were treated with ACC (1 mM), MeJA (100 μM), and MG132 (50 μM) for 6 h. Nuclear extracts were incubated with biotin-labeled ERE and GCC box oligonucleotide probes in EMSA. F, Effect of ACC and MeJA co-treatments on DNA binding of ORA59. Six-week-old plants were treated with ACC (1 mM), MeJA (100 μM), and a combination of ACC (1 mM) and MeJA (100 μM) for 6 h. Nuclear extracts were incubated with biotin-labeled ERE and GCC box oligonucleotide probes in EMSA. G, GUS reporter assays showing the effect of ACC and MeJA co-treatments on the expression of the GUS reporter gene driven by synthetic promoters of 4xERE and 4xRAV, and their mutant versions 4xmERE and 4xmRAV. The left part illustrates synthetic promoters. Transfected Col-0 and *ora59* protoplasts were treated with mock (water), ACC (200 μM), MeJA (20 μM), and a combination of ACC (200 μM) and MeJA (20 μM) for 6 h. Values represent means ± SD (*n* = 3 biological replicates). Asterisks indicate significant differences from mock treatment as determined by one-way ANOVA with Tukey test (\**P* < 0.05; \*\**P* < 0.01; \*\*\**P* < 0.001). In (B–F), ORA59 levels (input) in nuclear extracts were determined by immunoblotting with anti-GFP and anti-Histone H3 antibodies. Histone levels served as a control. In (B and D–F), to assess the phosphorylation status of ORA59, nuclear extracts were incubated with an anti-GFP antibody and the immunoprecipitated ORA59-GFP proteins were subjected to immunoblotting with anti-GFP and anti-phospho-Ser/Thr (pS/T) antibodies. IP, immunoprecipitation; GCC, GCC box; PP, phosphatase; A, ACC; J, MeJA.

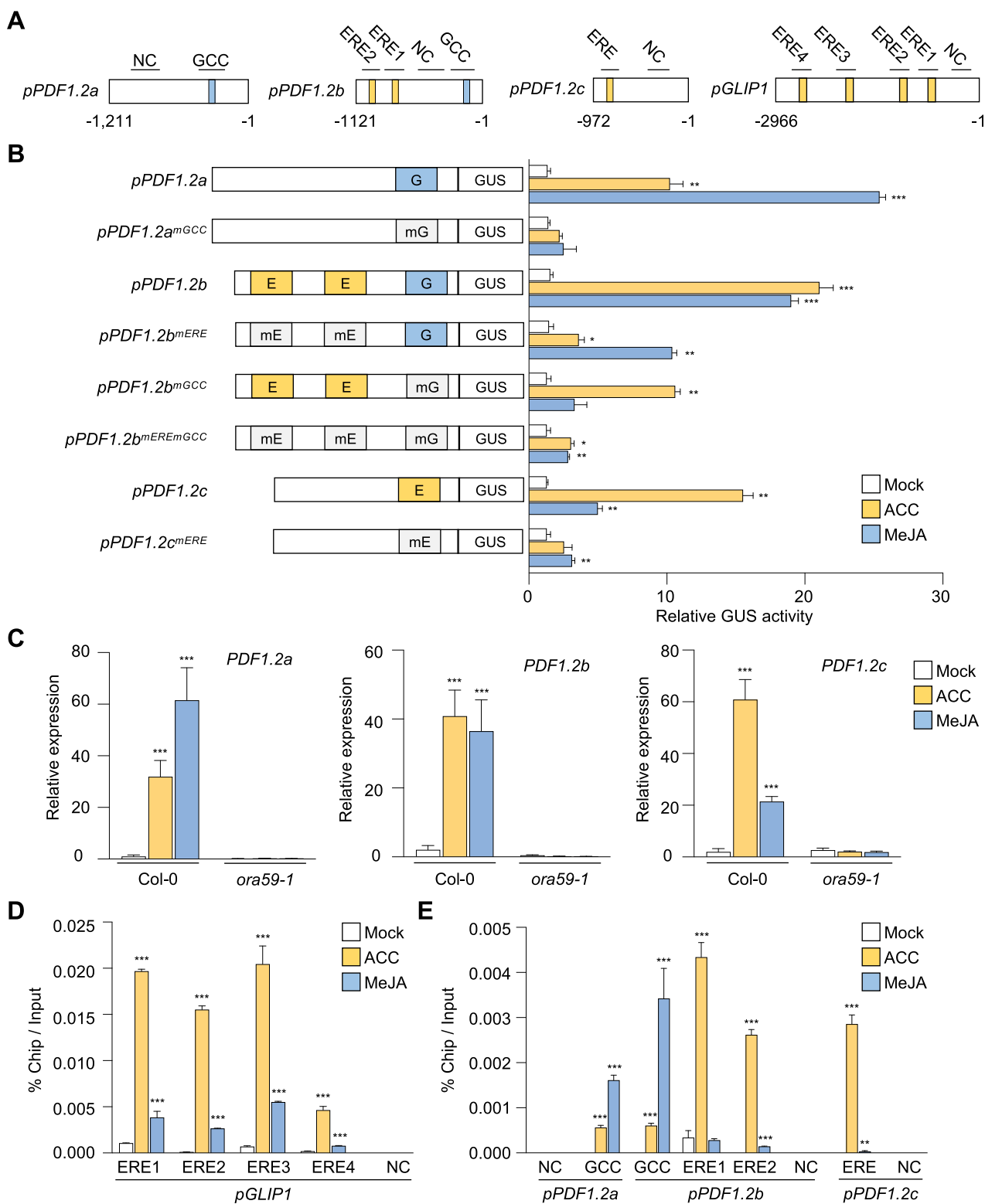


**Figure 4** ORA59 directly binds to ERE and GCC box of *GLIP1* and *PDF1.2* promoters in ACC- and JA-dependent manners. A, Schematic diagram of the ERE and GCC box elements in *PDF1.2* and *GLIP1* promoters. B, GUS reporter assays showing the ACC- and MeJA-induced expression of the GUS reporter gene driven by native or ERE/GCC box-mutated *PDF1.2a*, *b*, and *c* promoters. The left panel illustrates ERE and GCC box mutations of *PDF1.2a*, *b*, and *c* promoters. E, ERE; G, GCC box; mE, mutated ERE; mG, mutated GCC box. Transfected protoplasts were treated with mock (water), ACC (200  $\mu$ M), and MeJA (20  $\mu$ M) for 6 h. C, Analysis of *PDF1.2a*, *b*, and *c* expression in ACC- and MeJA-treated plants. D and E, ChIP-qPCR analysis for in vivo binding of ORA59 to ERE and GCC box sequences in the *GLIP1* (D) and *PDF1.2* (E) promoters. Chromatins from ACC- and MeJA-treated 35S:ORA59-GFP leaves were immunoprecipitated with an anti-GFP antibody. The enrichment of target element sequences is displayed as the percentage of input DNA. In (C–E), six-week-old plants were treated with ACC (1 mM) and MeJA (100  $\mu$ M) for 6 h. NC indicates the negative control region without ERE and GCC box sequences. Values represent means  $\pm$  SD ( $n = 3$  biological replicates). Asterisks indicate significant differences from mock treatment as determined by one-way ANOVA with Tukey test (\* $P < 0.05$ ; \*\* $P < 0.01$ ; \*\*\* $P < 0.001$ ).

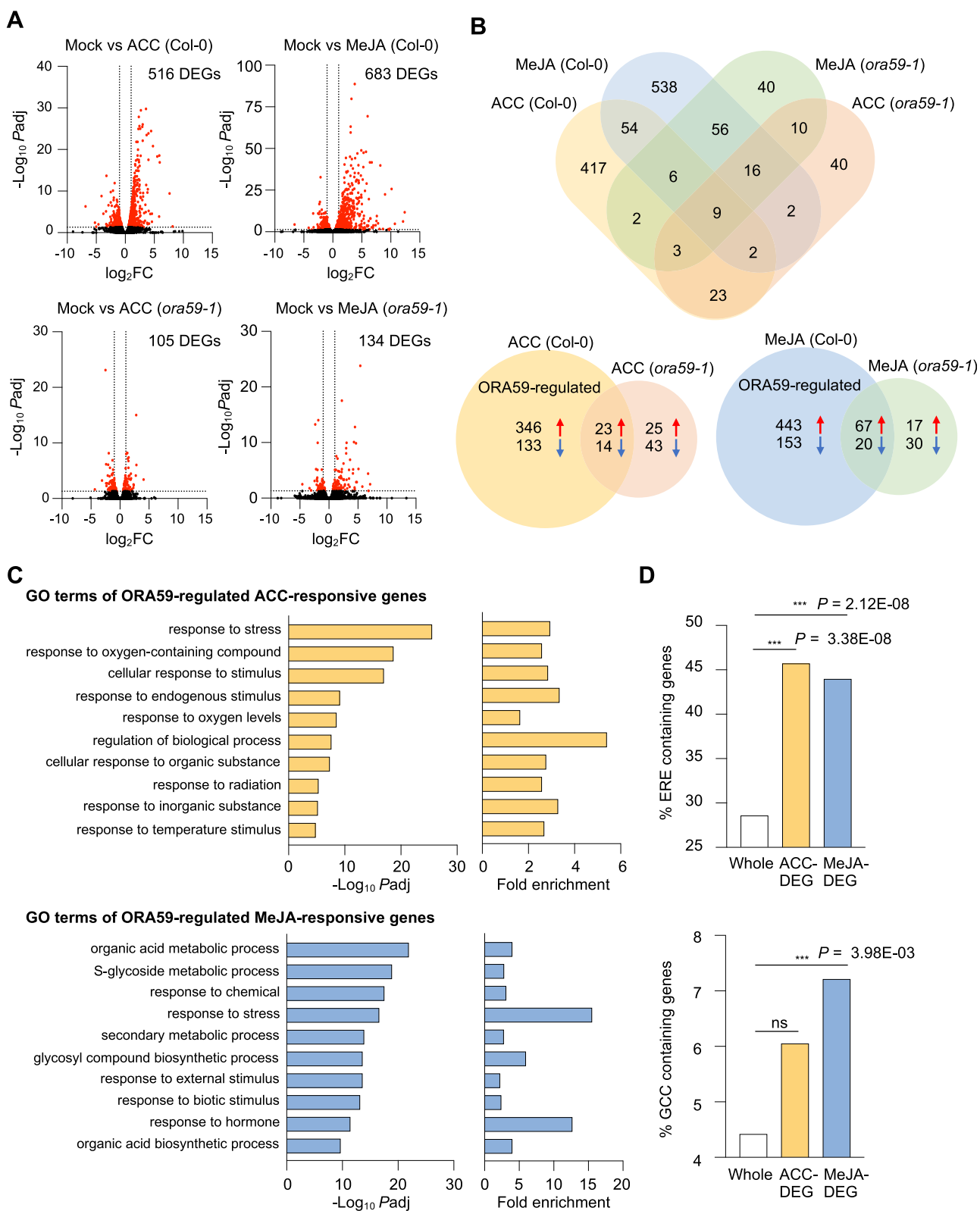


**Figure 5** Identification ORA59-regulated ET- and JA-responsive genes by RNA-seq analysis. A, Volcano plots of DEGs between mock and ACC/MeJA treatments in Col-0 and *ora59* plants. Cutoff values ( $P_{adj} = 0.05$  and  $|\log_2 FC| = 1$ ) are indicated by dashed lines. The red dots represent significantly upregulated and downregulated DEGs. B, Venn diagrams for DEGs between mock and ACC/MeJA treatments in Col-0 and *ora59* plants. C, GO enrichment analysis of ORA59-regulated DEGs. The 10 most significantly ( $FDR < 0.05$ ) enriched GO terms in the BP are presented for ACC- and MeJA-responsive genes. D, Analysis of the occurrence and enrichment of ERE and GCC box in promoters of ORA59-regulated ACC- and MeJA-responsive genes relative to whole Arabidopsis genes. The occurrence of ERE (AWTTCAAA) and GCC box (GCCGCC) sequences was analyzed using the regulatory sequence analysis tool. Statistical significance of enrichment was determined by Fisher's exact test (\*\* $P < 0.001$ ). Whole, whole Arabidopsis genes; ns, not significant.

RT-qPCR analysis (Supplemental Table S5). Toward isolating ORA59 target genes involved in the immune response, the expression of selected genes was assessed in 35S:ORA59-GFP and *B. cinerea*-treated Col-0 plants, among which eight ACC-responsive ( $|\log_2 \text{FC}| \geq 4$ ) and seven MeJA-responsive ( $|\log_2 \text{FC}| \geq 4$ ) genes were chosen to further investigate their functions in disease resistance (Figure 6A; Supplemental Figure S9).

We performed tobacco rattle virus (TRV)-based virus-induced gene silencing (VIGS) in Arabidopsis Col-0 (Burch-Smith et al., 2006; Ahn et al., 2015). TRV2 vector (control

and VIGS constructs carrying DNA fragments of 15 genes were transformed into *Agrobacterium*, which was followed by infiltration into true leaves of seedlings. Phenotypes of VIGS plants and transcript levels of target genes were determined in rosette leaves at 19- to 21-d post-infiltration. Consistent with previous observations (Burch-Smith et al., 2006), silencing of *PHYTOENE DESATURASE (PDS)*, used as a marker of VIGS, caused photo-bleaching of leaves and reduction of *PDS* expression compared to the TRV2 control (Supplemental Figure S10). All VIGS plants were successfully generated with >90% reduction in gene expression,

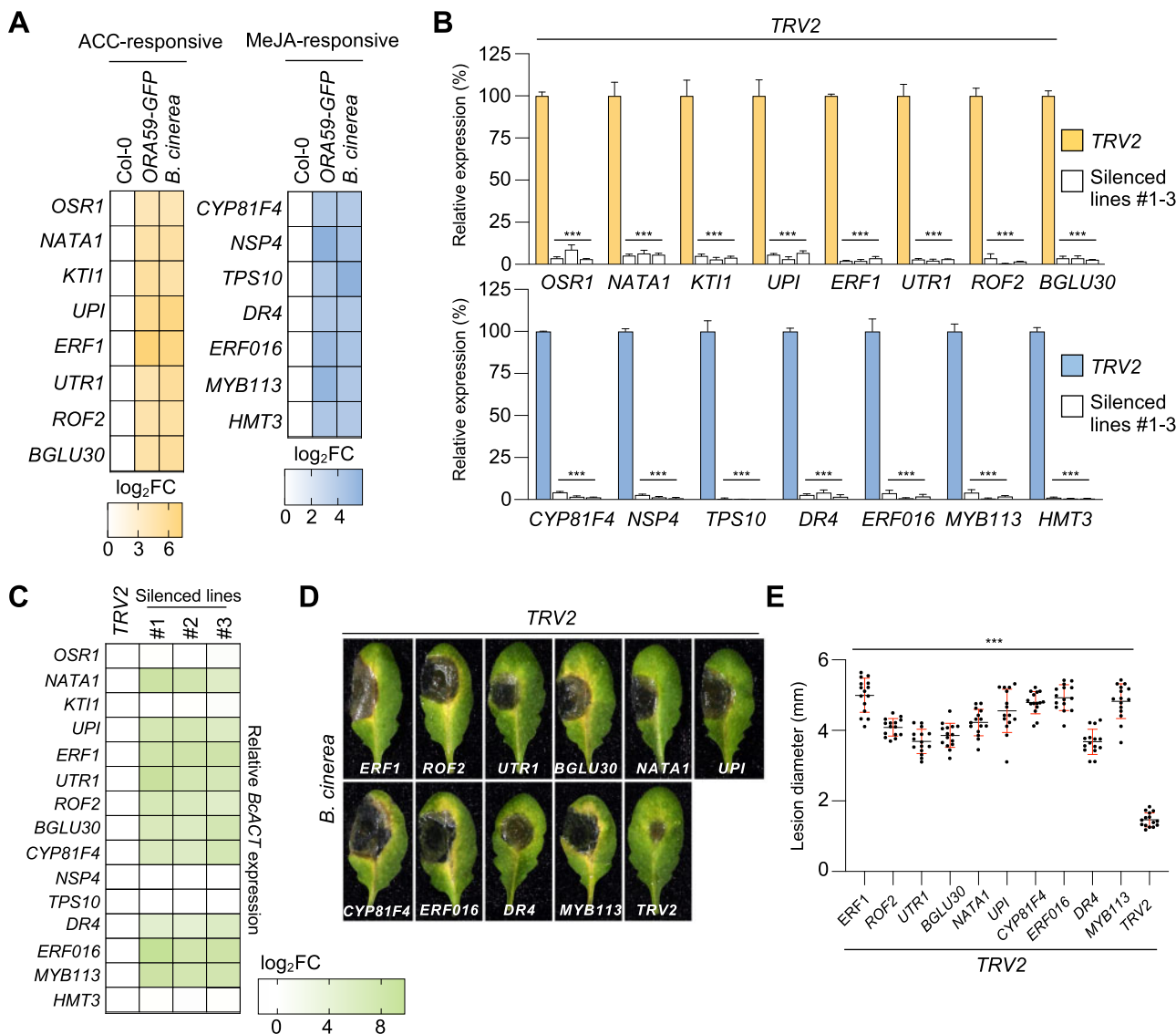


**Figure 6** Identification of immunity-associated ORA59 target genes. A, Heatmap showing the transcriptional levels of the most expressed DEGs in 35S:ORA59-GFP and *B. cinerea*-treated Col-0 plants relative to Col-0 plants. ACC-responsive eight ( $|\log_2 \text{FC}| \geq 4$ ) and MeJA-responsive seven ( $|\log_2 \text{FC}| \geq 4$ ) genes were selected for VIGS analysis. B, RT-qPCR analysis of the suppression of selected gene expression by VIGS. The transcript levels of selected genes in VIGS plants were determined relative to TRV2 control plants. Values represent means  $\pm$  SD ( $n = 3$  biological replicates). C, Heatmap showing the abundance of *B. cinerea* ACTIN (*BcACT*) gene relative to Arabidopsis TUBULIN 2 (*AtTU2*) in *B. cinerea*-treated TRV2 control and VIGS plants. D and E, Disease symptoms (D) and lesion diameters (E) in *B. cinerea*-treated TRV2 control and VIGS leaves. Values represent means  $\pm$  SD ( $n = 15$  infected leaves). In (C–E), TRV2 control and VIGS plants were treated with 5- $\mu$ L droplets of *B. cinerea* spore suspensions ( $5 \times 10^5$  spores  $\text{mL}^{-1}$ ) for 2 d. Asterisks indicate significant differences from the TRV2 control (B and E) as determined by one-way ANOVA with Tukey test ( $***P < 0.001$ ).

compared to the TRV2 control, and therefore challenged with *B. cinerea* (Figure 6B). Disease development, lesion size, and abundance of fungal actin gene were determined in the infected leaves (Figure 6, C–E). It was observed that susceptibility is increased by VIGS of 10 genes, i.e. ACC-responsive 6 and MeJA-responsive 4 genes, encoding ERF1, ROTAMASE FKBP 2 (ROF2)/FK506-BINDING PROTEIN 65 (FKBP65), UDP-GLUCOSE/GALACTOSE TRANSPORTER 1 (UTR1), BETA GLUCOSIDASE 30 (BGLU30)/DARK INDUCIBLE 2 (DIN2), N-ACETYLTRANSFERASE ACTIVITY 1 (NATA1), UNUSUAL SERINE PROTEASE INHIBITOR (UPI), CYTOCHROME P450, FAMILY 81, SUBFAMILY F, POLYPEPTIDE 4 (CYP81F4), ERF016, DROUGHT-REPRESSED 4 (DR4), and MYB DOMAIN PROTEIN 113 (MYB113). Consistently, the expression of these genes was significantly reduced in *ora59* plants compared to Co-0, in response to *B. cinerea* infection, suggesting that they function downstream of ORA59 in disease resistance (Supplemental Figure S11). Five other genes displayed no altered responses to *B. cinerea* after VIGS, perhaps because they are not related to disease resistance or it is attributed to genetic redundancy.

The isolated ORA59 target genes were scanned for the presence of ERE and GCC box in their promoters. Whereas 3 out of 10 genes had none of these elements, the other ACC- and MeJA-responsive genes contained one or more ERE and/or GCC box elements in the promoters (Figure 7A). We carried out ChIP-qPCR analyses using 35S:ORA59-GFP plants to determine whether ERE- and GCC box-containing genes are regulated by direct binding of ORA59 to their promoters. ChIP assays showed that ORA59 binding is enriched at ERE- and GCC box motifs of the promoters, indicating that they are direct targets of ORA59. ORA59 target genes were then analyzed for their ACC- and MeJA-responsive expression (Figure 7B). Among them, ACC- and MeJA-responsive genes were expressed more strongly by ACC and MeJA, respectively, than by the other, and their expression was induced synergistically by ACC and MeJA co-treatments. These results together suggest that ORA59 modulates immune responses to necrotrophic pathogens through regulation of target genes with diverse activities (Figure 7C).

## Discussion

Phytohormone signaling and crosstalk are critical for regulating plant immune responses. In particular, JA and ET have been identified as defense signals required for resistance against necrotrophic pathogens (Dong, 1998; Pieterse et al., 2009; Zhu, 2014). Upon pathogen infection, JA and ET are rapidly synthesized and work together, forming signaling networks that involve interactions among signaling components (Koornneef and Pieterse, 2008; Yang et al., 2015). Given that hormone signaling evokes output responses through gene regulation, JA and ET induce the expression of defense genes, such as *PDF1.2*, in a synergistic and interdependent manner (Thomma et al., 1998; Thomma et al., 1999; Koornneef and Pieterse, 2008). In this context, we observed an overlap between JA- and ET-responsive genes, but

on the other hand, other subsets of genes were differentially regulated by JA and ET, which was also described previously (Schenk et al., 2000).

JA/ET-mediated gene transcription typically occurs through the action of ERFs, among which ERF1 and ORA59 regulate *PDF1.2* expression by binding to GCC box and have been considered as integrators of JA and ET signaling (Lorenzo et al., 2003; Pre et al., 2008; Zarei et al., 2011). While ERF1 and ORA59 have been shown to regulate gene expression commonly in JA and ET pathways, questions are raised about how they respond differently to each hormone to induce JA- and ET-specific gene expression. In this study, we identified the poorly characterized ERE as an ORA59-binding cis-element, in addition to GCC box. EMSA, GUS reporter assays, and ChIP-qPCR analysis demonstrated that JA and ET enhance protein stability, and DNA binding and transactivation activities of ORA59 with differential preferences for GCC box and ERE, respectively. While supporting this, ORA59 regulated genes of different functional categories in JA and ET pathways, as shown by RNA-seq and GO analysis. An intriguing observation is that gene expression and transcription through ERE and GCC box with preferences for ACC or JA showed a synergistic increase when exposed to ACC and JA simultaneously. JA- and ET-mediated delicate gene regulation may be necessary for temporal and spatial transcriptional reprogramming to efficiently develop defense responses to necrotrophic pathogens, as revealed by temporal and spatial analysis of transcriptomic changes during Arabidopsis–*B. cinerea* interaction (Mulema and Denby, 2012; Windram et al., 2012). Our results provide insights into the molecular basis of how JA and ET modulate ORA59 to cooperatively and differentially regulate gene expression and to accomplish the fine-tuning of immune responses (Figure 7C).

EIN3 functions as a positive regulator of *ERF1* and *ORA59* expression (Solano et al., 1998; Zhu et al., 2011; Zander et al., 2012). JA- and ET-mediated induction of *ERF1* and *ORA59* was abolished in *ein3 eil1* mutant, and *ORA59* promoter activity was increased by *EIN3* overexpression. In addition, *EIN3* directly bound to the *ERF1* promoter, indicating that *ERF1* is the target gene of *EIN3*. Two different nucleotide sequences, TACAT and TTCAAA, have been identified as the *EIN3*-binding site (EBS) in the promoters of several *EIN3*-regulated genes, such as *ERF1*, *EBF2*, *PROTOCHLOROPHYLLIDE OXIDOREDUCTASE A and B (PORA/B)*, *HOOKLESS 1 (HLS1)*, and *microRNA164 (miR164)* (Solano et al., 1998; Konishi and Yanagisawa, 2008; Zhong et al., 2009; An et al., 2012; Li et al., 2013; Huang et al., 2020), and here they will be referred to as EBS1 and EBS2, respectively. In the course of this work, we have recognized that the EBS2, TTCAAA, is part of the ERE sequence AWTTCAAA, and this is especially true for the EBS2 in *PORB* and *HLS1* promoters. Therefore, we wonder whether *EIN3*-regulated genes containing the EBS2 in their promoters, which overlap with ERE, are also targets of ORA59, and whether ORA59 is implicated in other cellular processes, such as light signaling and seedling development.

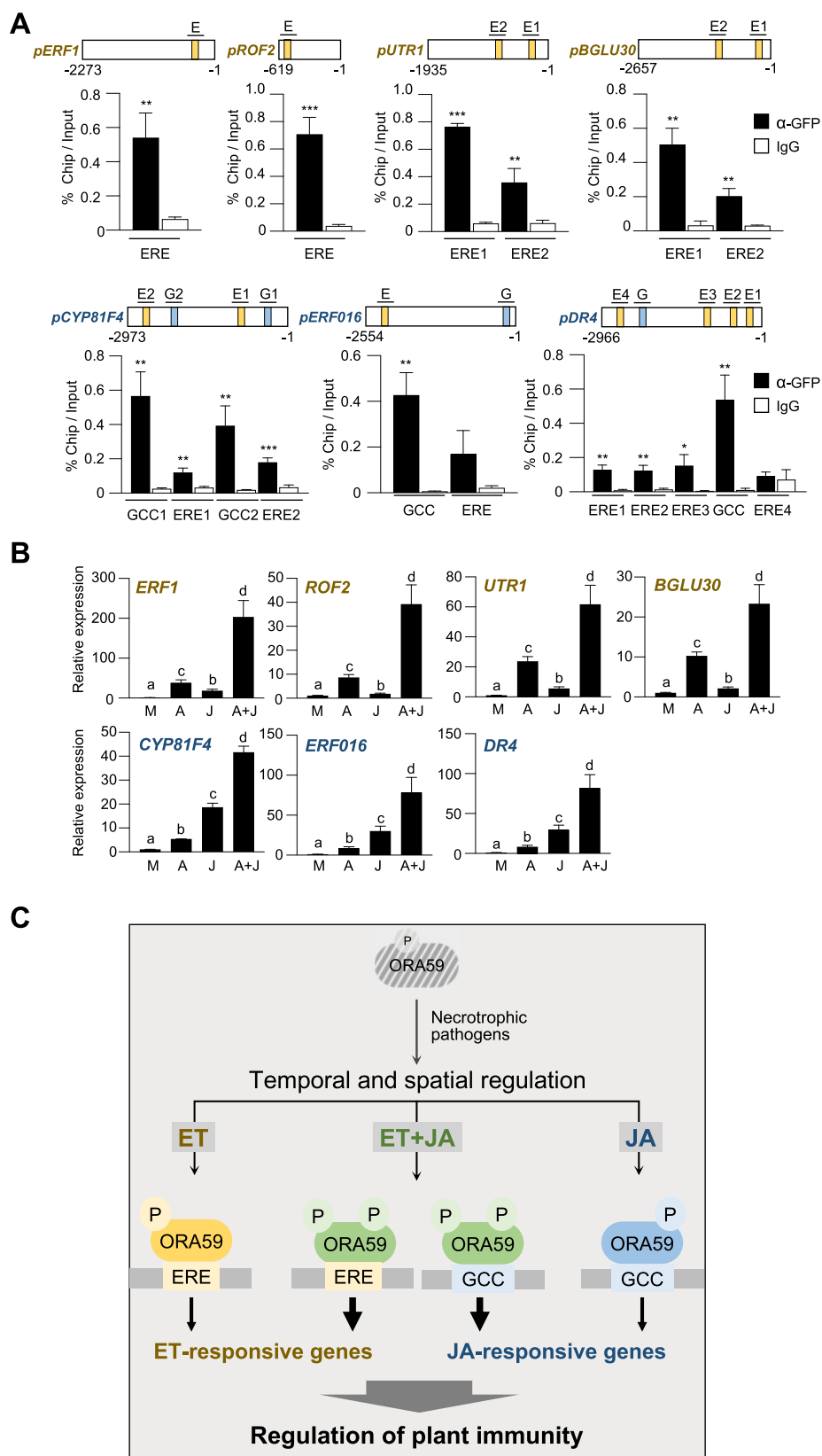


**Figure 7** ORA59 target genes show preferential and synergistic induction by ACC and JA. **A**, ChIP-qPCR analysis for *in vivo* binding of ORA59 to ERE and GCC box sequences in ORA59 target gene promoters. Chromatins from 35S:ORA59-GFP leaves were immunoprecipitated with an anti-GFP antibody using pre-immune IgG as a negative control. The enrichment of target element sequences is displayed as the percentage of input DNA. Values represent means  $\pm$  SD ( $n = 3$  biological replicates). E, ERE; G, GCC box. **B**, RT-qPCR analysis of ORA59 target gene expression in response to ACC, MeJA, and a combination of ACC and MeJA. Six-week-old Col-0 and mutant plants were treated with mock (water), ACC (1 mM), MeJA (100  $\mu$ M), and a combination of ACC (1 mM) and MeJA (100  $\mu$ M) for 6 h. M, mock; A, ACC; J, MeJA. **C**, Model for the mechanism of ET- and JA-responsive gene

It may be possible that EIN3 and ORA59 share and co-regulate certain target genes, which is supported by the evidence that EIN3 and ORA59 proteins interact together (He et al., 2017).

In our RNA-seq analysis, ERF1 was isolated as an ORA59-regulated ET-responsive gene. In addition to the previously identified EBS2 (Solano et al., 1998), the *ERF1* promoter has a separate ERE, to which ORA59 directly bound as determined by ChIP analysis, implying that ORA59 is the upstream regulator of *ERF1*. A previous study showed that *ERF1* expression is decreased in *ora59* mutant (Zander et al., 2014). Conversely, ORA59 expression was largely increased in *ERF1*-overexpressing plants (Van der Does et al., 2013). In the EMSA analysis, ERF1 exhibited binding activity to ERE sequences. Given that the ORA59 promoter contains both ERE and GCC box, ORA59 and ERF1 may activate each other via a positive feedback loop. Furthermore, ERF1 bound to another stress-responsive element DRE/CRT during abiotic stress responses, as shown in a previous study (Cheng et al., 2013). This and our data suggest that ERFs, including ERF1 and ORA59, may bind to distinct types of cis-elements, depending on hormone and stress stimuli. On the other hand, studies have shown that other transcription factors, TGA2/4/6 (class II TGAs) and WRKY33, positively regulate ORA59 expression in response to ACC and *B. cinerea* infection through binding to the TGA binding site TGACGT and W-box TTGAC(C/T) in the ORA59 promoter, respectively (Birkenbihl et al., 2012; Zander et al., 2014). Further investigation is needed on how ET/JA-regulated EIN3, ORA59, and ERF1, and other types of transcription factors, such as TGAs and WRKYs, interact and coordinately regulate gene expression in the transcriptional and protein interaction networks.

Protein phosphorylation regulates the function of transcription factors by modulating DNA binding, transcriptional activity, protein stability, cellular localization, and protein-protein interactions. Many reports provide evidence that ERFs are regulated by phosphorylation (Licausi et al., 2013; Huang et al., 2016; Phukan et al., 2017). Phosphorylation of the tomato (*Lycopersicon esculentum*) ERF Pti4 by Pto kinase enhanced Pti4 binding to GCC box, increasing the expression of GCC box-containing *PR* genes (Gu et al., 2000). MITOGEN-ACTIVATED PROTEIN KINASE (MAPK/MPK) cascades have been implicated in ERF phosphorylation. When phosphorylated by BLAST AND WOUND-INDUCED MAPK1 (BWMK1), the rice ET-RESPONSIVE ELEMENT-BINDING PROTEIN 1 (OsEREBP1) showed enhanced DNA

binding activity to GCC box, and concomitantly, the increased GCC box-driven transcription (Cheong et al., 2003). Transactivation by the tobacco NtERF221 (originally designated as ORC1) was positively affected by a MAPK kinase, JA-FACTOR-STIMULATING MAPKK1 (De Boer et al., 2011). The Arabidopsis ERF6 served as an MPK substrate, and its protein stability and nuclear localization were increased by MPK3/MPK6-mediated ERF6 phosphorylation (Meng et al., 2013; Wang et al., 2013). In this study, we showed that ORA59 phosphorylation is elevated in plants treated with either ACC or MeJA. ORA59 activated through ACC and JA signals had differential preferences for ERE and GCC box, in addition to enhanced DNA binding, which was eliminated by phosphatase-mediated dephosphorylation of ORA59. Likewise, ORA59 proteins which accumulated in MG132-treated plants showed a similar level of binding to these elements. These results suggest that phosphorylation regulates both affinity and specificity of ORA59 for DNA sequences. Furthermore, recombinant ORA59 proteins with deletion of the N- and C-terminal parts showed differential GCC box- and ERE-binding activities, suggesting that ORA59 may form distinct structures with different affinities for ERE and GCC box, and this may be regulated by hormone-dependent differential phosphorylation events (Figure 7C). We speculate that ORA59 may be phosphorylated at different Ser/Thr residues in the ET and JA pathways, leading to differential binding of ORA59 to ERE and GCC box. When ORA59 is activated by both ET and JA, Ser/Thr residues phosphorylated specifically by each hormone may be all phosphorylated. As a result, ORA59 may lose specificity for ET and JA, rather leading to a synergistic increase in ET- and JA-responsive gene expression. In the future study, it is important to investigate whether ORA59 phosphorylation is induced by different kinases in ET- and JA-dependent ways and whether it modulates the structure and activity of ORA59. A combination of ACC and MeJA treatments further increased the level of phosphorylation, but not that of DNA binding activity of ORA59, suggesting that ORA59 phosphorylation may be involved in ET and JA synergy at the level of transcriptional activation, e.g. interaction with other cofactors/transcription factors and transcription machinery components.

Gene expression, VIGS, and ChIP analysis led to the identification of direct target genes of ORA59, *ERF1*, *ROF2/FKBP65*, *UTR1*, *BGLU30/DIN2* as ACC-responsive genes, and *CYP81F4*, *DR4*, and *ERF016* as MeJA-responsive genes, and indirect target genes, *NATA1*, *UPI*, and *MYB113*. These ORA59 target

#### Figure 7 Continued

regulation by ORA59. Pathogenic infection triggers ET and JA biosynthesis, likely with different kinetic patterns, resulting in the temporal and spatial activation of ET and JA signaling. ET and JA pathways lead to phosphorylation, possibly at different Ser/Thr residues, which requires further verification, and stabilization of ORA59. This enhances DNA binding and transactivation activities of ORA59 with differential preference for ERE and GCC box. Consequently, distinct sets of genes are regulated by ORA59 in ET and JA pathways. When simultaneously exposed to ET and JA, ORA59 undergoes increased phosphorylation and more strongly activates ET- and JA-responsive genes. In this way, ET- and JA-activated ORA59 differentially and synergistically regulate target genes and fine-tunes immune responses. In (A and B), significance differences are indicated by asterisks (\* $P < 0.05$ ; \*\* $P < 0.01$ ; \*\*\* $P < 0.001$ ) compared to the pre-immune IgG control (A) and by different letters ( $P < 0.05$ ) (B) as determined by one-way ANOVA with Tukey test.

genes are clustered into four functional groups. First, *ERF1*, *ERF016*, and *MYB113* encode transcription factors, which are involved in the regulation of defense gene expression. *ERF1* has been well characterized to enhance *PDF1.2* expression and disease resistance (Zarei et al., 2011). *ERF016* bound to GCC box of the *PDF1.2* promoter and *erf016* mutants displayed a significant increase in susceptibility to *B. cinerea* (Ou et al., 2011; Hickman et al., 2017). *MYB113* expression was much reduced in *ora59* mutant, suggesting that *MYB113* functions downstream of *ORA59* (Zander et al., 2014). Second, *DR4* and *UPI* encode protease inhibitors implicated in resistance to necrotrophic fungi (Gosti et al., 1995; Brodersen et al., 2006; Laluk and Mengiste, 2011). Third, *BGLU30/DIN2*, *CYP81F4*, and *NATA1* function in secondary metabolic pathways. *BGLU30/DIN2*, encoding a  $\beta$ -glucosidase, and *CYP81F4*, encoding a cytochrome P450 monooxygenase, showed activities associated with glucosinolate metabolism (Pfalz et al., 2011; Morikawa-Ichinose et al., 2020; Zhang et al., 2020). Glucosinolates and their breakdown products function in defense against pathogens (Bednarek, 2012), supporting the possibility that *BGLU30* and *CYP81F4* may play a role in plant immunity. *NATA1* was identified as an acetyltransferase that acetylates ornithine and putrescine in response to coronatine, JA, and *P. syringae* infection (Adio et al., 2011; Lou et al., 2016). Fourth, *ROF2/FKBP65*, encoding a peptidyl-prolyl cis-trans isomerase, and *UTR1*, encoding a nucleotide sugar transporter, are involved in protein folding and endoplasmic reticulum (ER) quality control processes. Knockout or overexpression of *ROF2/FKBP65* decreased or increased resistance against *P. syringae*, respectively (Pogorelko et al., 2014). *UTR1*, required for the transport of UDP-glucose into the ER, may be involved in plant immunity, because proper folding of immune receptors and PRRs relies on the ER quality control system (Reyes et al., 2006; Eichmann and Schafer, 2012). Further studies on the functions of *ORA59* target genes will improve our understanding of the ET–JA signaling network and involving components in the regulation of plant immunity.

## Materials and methods

### Plant materials and growth conditions

*Arabidopsis* (*A. thaliana*; ecotype Columbia, Col-0) plants were grown at 23°C under long-day conditions in a 16-h light/8-h dark cycle. The mutant lines used in this study are *glip1-1* (Oh et al., 2005), *ein2-1* (Roman and Ecker, 1995), *ein3-1eil1-1* (Alonso et al., 2003), *ora59* (CS\_405772), and *coi1* (SALK\_095916). Homozygous lines were selected by PCR and sequence analysis using gene-specific primers (Supplemental Table S6). To generate 35S:*ORA59-GFP* plants, the *ORA59* coding region was cloned into the pCHF3-GFP binary vector under the control of the CaMV 35S promoter. To generate *pGLIP1:GUS* and *pGLIP1<sup>mERES</sup>:GUS* plants, the *GLIP1* promoter region (–1 to –2966 bp) was amplified from *Arabidopsis* gDNA by PCR and cloned into the pBI121 vector containing a *GUS* gene. ERE mutations in the *GLIP1*

promoter were generated by site-directed mutagenesis using primers in Supplemental Table S6. For *pGLIP1:GLIP1-GFP* and *pGLIP1<sup>mERES</sup>:GLIP1-GFP* plants, the *GLIP1* coding region was cloned into the pCAMBIA1300 vector containing a *GFP* gene, and then *pGLIP1* and *pGLIP1<sup>mERES</sup>* were inserted upstream of *GLIP1-GFP* in the pCAMBIA1300 vector. The constructs were transformed into *Agrobacterium tumefaciens* GV3101 and then introduced into Col-0 and *glip1-1* plants using the floral dip method (Clough and Bent, 1998).

### Plant treatments

For pathogen infection, *B. cinerea* and *A. brassicicola* were grown on potato dextrose agar plates for 2 weeks, and their spores were harvested and incubated in half-strength potato dextrose broth for 2 h prior to inoculation as previously described (Broekaert et al., 1990). Six-week-old leaves were inoculated with 5- $\mu$ L droplets of spore suspensions ( $5 \times 10^5$  spores mL<sup>-1</sup>). Fungal growth was assessed by qPCR for the abundance of *A. brassicicola* *CUTINASE A* (*AbCUTA*) and *B. cinerea* *ACTIN* (*BcACT*) genes relative to *Arabidopsis* *TUBULIN 2* (*AtTU2*). Lesion size was determined by measuring the diameter of the necrotic area. For chemical treatments, 6-week-old plants were sprayed with 0.01% (v/v) Silwet L-77 containing 1 mM SA, 1 mM ACC, 100  $\mu$ M MeJA, 50  $\mu$ M MG132, and 100  $\mu$ M CHX or incubated with 10 ppm ET in hydrocarbon-free air. The treated plants were maintained at 100% humidity for the indicated times.

### Transient expression assays

For transient assays in *Arabidopsis* protoplasts, effector and reporter constructs were generated. For effector constructs, coding regions of *ORA59*, *RAP2.2*, and *CPL3* were amplified from the *Arabidopsis* cDNA library by PCR and cloned into the pUC18 vector for the expression of hemagglutinin (HA)-tagged proteins in protoplasts (Cho and Yoo, 2011). For gene promoter–reporter constructs, promoter regions of *GLIP1*, *PDF1.2a*, *PDF1.2b*, and *PDF1.2c* were amplified from *Arabidopsis* gDNA by PCR and cloned into the pBI221 vector containing a *GUS* gene. Mutations of ERE and GCC box elements in the promoter regions were generated by site-directed mutagenesis using primers in Supplemental Table S6. For synthetic promoter–reporter constructs, four copies of the native ERE or GCC box and four copies of respective mutated versions were fused with the minimal *GLIP1* promoter (–1 to –122 bp) and cloned into the pBI221 vector containing a *GUS* gene. *Arabidopsis* mesophyll protoplasts were isolated and transfected as previously described (Yoo et al., 2007). Isolated protoplasts ( $2 \times 10^4$ ) were transfected with a reporter DNA (20  $\mu$ g) alone or together with an effector DNA (20  $\mu$ g). As previously described (Jefferson et al., 1987), *GUS* activity was measured fluorometrically using 4-methylumbelliferyl- $\beta$ -D-glucuronide as substrate. The firefly LUCIFERASE (*LUC*) expressed under the control of the CaMV 35S promoter was used as an internal control, and the activity was measured using the luciferase assay system



(Promega). Relative GUS activities were normalized with respect to the LUC activity.

### Histochemical GUS staining

GUS staining was performed as previously described (Lee et al., 2017). Rosette leaves were incubated in a staining buffer (50 mM sodium phosphate, pH 7.0, 0.5 mM  $K_3Fe(CN)_6$ , 0.5 mM  $K_4Fe(CN)_6$ , 10 mM EDTA, and 0.2% Triton X-100) containing 4 mM 5-bromo-4-chloro-3-indolyl- $\beta$ -D-glucuronide (X-Gluc) for 16 h at 37°C. Stained leaves were cleared by several washes with 70% ethanol.

### Yeast one-hybrid (Y1H) screening

Y1H screening was performed as previously described (Welchen et al., 2009). To obtain a yeast strain carrying the ERE sequence in front of the *HIS3* reporter gene, three tandem repeats of ERE were cloned into the pHIS3-NX vector, and the 3xERE-*HIS3* cassette was cloned into the pINT vector, which confers resistance to the antibiotic G418. The clone in pINT1 was introduced into the yeast strain Y187. Alternatively, the 3xERE was placed in front of the *lacZ* reporter gene contained in the pLacZi vector (Clontech). Transcription factors interacting with the ERE sequence were identified using a DNA library carrying a 1,050 Arabidopsis transcription factor ORFeome collection in the prey vector pDEST22 (Invitrogen). For Y1H screening, plasmid DNA from the library (10  $\mu$ g) was introduced into yeast and a total of  $2 \times 10^6$  transformants were plated on SD-Trp-His medium containing 0.2 mM 3-AT. The resulting putative positive clones were streaked on fresh SD-Trp-His + 0.2 mM 3-AT medium to purify colonies. The plasmid DNAs containing ORFs were rescued and retransformed into yeast for confirmation.

### Protein expression and purification

The full-length coding regions of *ORA59*, *RAP2.2*, *CPL3*, and the truncated regions of *ORA59* were PCR-amplified using gene-specific primers (Supplemental Table S6). The PCR products were cloned into the pMAL-x2X vector to generate proteins fused to the N-terminal MALTOSE-BINDING PROTEIN (MBP) and His-tag. *Escherichia coli* BL21(DE3) pLys cells were transformed with the constructs and cultured at 28°C. Protein expression was induced by the addition of 0.3 mM IPTG for 3 h at 28°C. The MBP/His-tagged proteins were purified using  $Ni^{2+}$ -NTA agarose (Qiagen) according to the manufacturer's instructions.

### Nuclear extraction

Five-week-old leaves were ground in liquid nitrogen and incubated in a nuclear extraction buffer (20 mM PIPES-KOH, pH 7.0, 10 mM KCl, 1.5 mM  $MgCl_2$ , 0.3% Triton X-100, 5 mM EDTA, 1 mM DTT, 1 M 2-methyl-2,4-pentandiol, 1 mM NaF, 1 mM  $Na_3VO_4$ , and protease inhibitor cocktail) on ice for 10 min. The material was filtered through one layer of Miracloth and spun at 1,000 g for 10 min at 4°C. After removing the supernatant, the pellet was resuspended in a buffer (20 mM PIPES-KOH, pH 7.0, 10 mM  $MgCl_2$ , 1%

Triton X-100, 1 mM DTT, 0.5 M hexylene glycol (2-methyl-2,4-pentandiol), 1 mM NaF, and 1 mM  $Na_3VO_4$ ), incubated on ice for 10 min, and then centrifuged at 1,000 g for 10 min at 4°C. To extract nuclear proteins, isolated nuclei were resuspended in an extraction buffer (20 mM HEPES, pH 8.0, 300 mM NaCl, 1 mM  $MgCl_2$ , 0.2 mM EDTA, 10% glycerol, 1% Triton X-100, 0.1% NP-40, 1 mM DTT, 1 mM NaF, 1 mM  $Na_3VO_4$ , and protease inhibitor cocktail), incubated with rotation for 30 min at 4°C, and then centrifuged at 15,000g for 20 min at 4°C. The supernatant was collected, and the protein concentration was determined before use. For phosphatase treatment, phosphatase inhibitors (NaF and  $Na_3VO_4$ ) were excluded from the extraction buffer, and extracted nuclear proteins were treated with lambda protein phosphatase (NEB) according to the manufacturer's instruction.

### Electrophoretic mobility shift assay (EMSA)

EMSA was performed using the LightShift Chemiluminescent EMSA kit (Thermo Scientific). Biotin-labeled oligonucleotides were synthesized by Macrogen (Korea). Purified proteins or nuclear extracts were incubated in 20 fM biotin-labeled oligonucleotide probes in 15  $\mu$ L of a binding buffer (10 mM Tris-HCl, pH 7.5, 40 mM KCl, 3 mM  $MgCl_2$ , 1 mM EDTA, 10% glycerol, 1 mM DTT, and 3  $\mu$ g poly(dI-dC)) for 30 min at room temperature (purified proteins) or at 4°C (nuclear extracts). In the supershift assay, nuclear extracts were pre-incubated with 1  $\mu$ g of anti-GFP antibody or pre-immune IgG prior to the addition of biotin-labeled oligonucleotide probes. The samples were resolved on 5% polyacrylamide (75:1 acrylamide:bis-acrylamide) gels. In the competition assay, purified *ORA59* proteins were incubated with the indicated excess amounts of oligonucleotide competitors for 15 min before the addition of biotin-labeled probes.

### Immunoblotting and immunoprecipitation

For immunoblotting, proteins were separated on 10%–12% SDS-polyacrylamide gels by SDS-gel electrophoresis and electro transferred onto nitrocellulose membranes. Membranes were incubated with anti-GFP (sc-9996, Santa Cruz Biotechnology), anti-Actin (ab197345, Abcam), anti-Histone H3 (ab1791, Abcam), and anti phospho Ser/Thr (ab17464, Abcam) antibodies. For immunoprecipitation, nuclear pellets were lysed in hypotonic buffer (20 mM HEPES, pH 7.9, 20 mM KCl, 1.5 mM  $MgCl_2$ , and 25% glycerol) and high-salt buffer (20 mM HEPES, pH 7.9, 800 mM KCl, 1.5 mM  $MgCl_2$ , 25% glycerol, and 1% NP-40) supplemented with protease inhibitor cocktail and incubated with rotation at 4°C. Lysates were cleared by centrifugation and incubated with an anti-GFP antibody for 2 h at 4°C. After an additional 2-h incubation with Protein G Agarose (20399, Thermo Scientific), beads were washed with wash buffer (20 mM Tris-HCl, pH 7.9, 150 mM KCl, 20% glycerol, 0.1 mM EDTA, and 0.1% NP-40) and bound proteins were eluted with  $2 \times$  sample buffer (100 mM Tris-HCl, pH 6.5, 20% glycerol, 4% SDS, 200 mM DTT, and 3 mM bromophenol

blue). Immunoblot bands were visualized using the enhanced chemiluminescence system (Amersham Biosciences).

### Gene expression analysis

Total RNAs were extracted using TRIzol reagent and reverse-transcribed into cDNAs using the PrimeScript RT reagent kit (TaKaRa). RT-qPCR was performed using KAPA SYBR FAST qPCR master mix (Kapa Biosystems) with gene-specific primers (Supplemental Table S6) on a LightCycler 480 system (Roche) according to the manufacturer's protocol. For transcript normalization, *Actin1* was used as a reference gene. Data were analyzed using LC480Conversion and LinRegPCR software (Heart Failure Research Center).

### RNA-seq data analysis

Total RNAs were extracted from leaves using RNeasy Plant Mini kit (Qiagen). The amount of RNAs was measured using Nanodrop (Thermo Scientific) and the quality was assessed using Bioanalyzer (Agilent Technologies) with an RNA Integrity Number value  $\geq 8$ . The RNA-seq libraries were prepared using the TruSeq RNA preparation kit V2 kit following the manufacturer's instructions. The 150-bp paired-end sequencing reads were generated on the Illumina NextSeq 550 System instrument platform. The low-quality base (base quality score  $< 20$ ) in the last position of the reads was trimmed and high-quality sequencing reads were subsequently aligned onto the *A. thaliana* reference genome (TAIR10) using HISAT2 (Kim et al., 2019). The raw number of reads mapped onto each transcript was quantified using StringTie (Pertea et al., 2015) and the counts per transcript were normalized based on the library size by DESeq2 (Love et al., 2014). The batch effect among samples was estimated by PCA and corrected by limma (Ritchie et al., 2015). Statistically significant DEGs were tested based on a negative binomial distribution using a generalized linear model. Enriched GO terms for DEGs were determined using the statistical overrepresentation test in PANTHER (<http://geneontology.org>). Gene lists were compared to all Arabidopsis genes in PANTHER using the GO BP dataset and binomial test with FDR correction.

### Chromatin immunoprecipitation (ChIP)

ChIP assays were performed as described previously (Lee et al., 2017). Five-week-old 35S:ORA59-GFP leaf tissues were fixed with 1% formaldehyde under vacuum, washed, dried, and ground to a fine powder in liquid nitrogen. The powder was suspended in M1 buffer (10 mM sodium phosphate, pH 7.0, 0.1 M NaCl, 1 M 2-methyl 2,4 pentanediol, 10 mM  $\beta$ -mercaptoethanol, and protease inhibitor cocktail). Nuclei were isolated from the filtrate by centrifugation at 1,000g for 20 min at 4°C and washed with M2 buffer (10 mM sodium phosphate, pH 7.0, 0.1 M NaCl, 1 M 2-methyl 2,4 pentanediol, 10 mM  $\beta$ -mercaptoethanol, 10 mM MgCl<sub>2</sub>, 0.5% Triton X-100, and protease inhibitor cocktail) and M3 buffer (10 mM sodium phosphate, pH 7.0, 0.1 M NaCl, 10 mM  $\beta$ -mercaptoethanol, and protease inhibitor cocktail). The crude nuclear pellet was resuspended in sonication buffer (10 mM

sodium phosphate, pH 7.0, 0.1M NaCl, 0.5% Sarkosyl, and 10 mM EDTA) and sonicated to obtain DNA fragments. The fragmented chromatin was transferred to IP buffer (50 mM HEPES, pH 7.5, 150 mM NaCl, 5 mM MgCl<sub>2</sub>, 10  $\mu$ M ZnSO<sub>4</sub>, 1% Triton-X 100, and 0.05% SDS). The precleared chromatin was incubated with IgG or GFP antibody (A11122, Thermo Scientific) for 2 h at 4°C. After an additional overnight incubation with Protein A Sepharose (20333, Thermo Scientific), beads were incubated in elution buffer (0.1M glycine, pH 2.8, 0.5 M NaCl, 0.05% Triton X-100). Primers for qPCR are listed in Supplemental Table S6.

### Virus-induced gene silencing

VIGS was performed as previously described (Burch-Smith et al., 2006). Coding regions of target genes were amplified and cloned into the pTRV2 vector. The constructs were transformed into *A. tumefaciens* strain GV3101, which was cultured in LB media containing 10 mM MES-KOH (pH 5.7), 200  $\mu$ M acetosyringone, 50 mg L<sup>-1</sup> gentamycin, and 50 mg L<sup>-1</sup> kanamycin overnight at 28°C. *Agrobacterium tumefaciens* cells were harvested, adjusted to an OD<sub>600</sub> of 1.5 in infiltration media (10 mM MES-KOH, pH 5.7, 10 mM MgCl<sub>2</sub>, and 200  $\mu$ M acetosyringone), and infiltrated into leaves of Arabidopsis seedlings at 15–17 d after germination. After 19–21 d, VIGS plants were treated with pathogens and silencing effects were verified in the systemic leaves by gene-specific primers (Supplemental Table S6).

### Statistical analysis

Statistical analyses were performed using GraphPad Prism (v. 8.0). Significant differences between experimental groups were analyzed by one-way ANOVA with Tukey's HSD test or unpaired Student's *t* test for multiple comparisons or single comparisons, respectively. Detailed information about statistical analysis is described in the Figure legends. Statistical significance was set at  $P < 0.05$ . All experiments were repeated three to five times with similar results.

### Accession numbers

Sequence data from this article can be found in the Arabidopsis Genome Initiative or GenBank/EMBL databases under the following accession numbers: ORA59 (AT1G06160), GLIP1 (AT5G40990), RAP2.2 (AT3G14230), CPL3 (AT4G01060), PDF1.2A (AT5G44420), PDF1.2B (AT2G26020), PDF1.2C (AT5G44430), OSR1(AT2G41230), NATA1 (AT2G39030), KTI1 (AT1G73260), UPI (AT5G43580), ERF1 (AT3G23240), UTR1 (AT2G02810), ROF2 (AT5G48570), BGLU30 (AT3G60140), CYP81F4 (AT4G37410), NSP4 (AT3G16410), TPS10 (AT2G24210), DR4 (AT1G73330), ERF016 (AT5G21960), MYB113 (AT1G66370), and HMT3 (AT3G22740).

### Supplemental data

The following materials are available in the online version of this article.

**Supplemental Figure S1.** RT-qPCR analysis of ET- and JA-responsive *GLIP1* expression.

**Supplemental Figure S2.** ERE is required for ET-responsive *GLIP1* expression.

**Supplemental Figure S3.** ERE is required for *GLIP1* expression during the immune response.

**Supplemental Figure S4.** Purification of recombinant ORA59, RAP2.2, CPL3, and truncated forms of ORA59.

**Supplemental Figure S5.** EMSA analysis of ERF1 to ERE sequences.

**Supplemental Figure S6.** Preparation of 35S:ORA59-GFP transgenic lines.

**Supplemental Figure S7.** ORA59 binding to ERE and GCC box is regulated in ET- and JA-dependent manners.

**Supplemental Figure S8.** EMSA supershift analysis of nuclear ORA59 proteins from 35S:ORA59-GFP plants.

**Supplemental Figure S9.** Heatmap showing the expression of up-regulated DEGs in 35S:ORA59-GFP plants and in response to *B. cinerea*.

**Supplemental Figure S10.** VIGS of *PHYTOENE DESATURASE (PDS)* in Col-0 plants.

**Supplemental Figure S11.** RT-qPCR analysis of VIGS target gene expression in *ora59* plants and in response to *B. cinerea*.

**Supplemental Table S1.** Putative cis-elements in the *GLIP1* promoter.

**Supplemental Table S2.** Candidate ERE-binding transcription factors from Y1H screening.

**Supplemental Table S3.** Raw data of RNA-seq and DEGs between mock and ACC/MeJA treatments.

**Supplemental Table S4.** GO enrichment analysis of ORA59-regulated ACC- and MeJA-responsive genes.

**Supplemental Table S5.** RT-qPCR analysis of ORA59-regulated ACC- and MeJA-responsive gene expression.

**Supplemental Table S6.** Primers used in this study.

## Acknowledgments

We are grateful to H. S. Pai (Yonsei University, Korea) for technical help with VIGS.

## Funding

This work was supported by a Korea University grant and National Research Foundation of Korea (NRF) grants (2018R1A5A1023599, 2021R1A2C1003213) from the Korean government (MSIP). J.C.H. acknowledges support from an NRF grant (2020R1A6A1A03044344) from the Korean government (MSIP).

*Conflict of interest statement.* The authors declare that there is no conflict of interest.

## References

- Adio AM, Casteel CL, De Vos M, Kim JH, Joshi V, Li B, Juery C, Daron J, Kliebenstein DJ, Jander G** (2011) Biosynthesis and defensive function of Ndelta-acetylornithine, a jasmonate-induced Arabidopsis metabolite. *Plant Cell* **23**: 3303–3318
- Ahn HK, Kang YW, Lim HM, Hwang I, Pai HS** (2015) Physiological functions of the COPI complex in higher plants. *Mol Cells* **38**: 866–875
- Alonso JM, Hirayama T, Roman G, Nourizadeh S, Ecker JR** (1999) EIN2, a bifunctional transducer of ethylene and stress responses in Arabidopsis. *Science* **284**: 2148–2152
- Alonso JM, Stepanova AN, Solano R, Wisman E, Ferrari S, Ausubel FM, Ecker JR** (2003) Five components of the ethylene-response pathway identified in a screen for weak *ethylene-insensitive* mutants in Arabidopsis. *Proc Natl Acad Sci USA* **100**: 2992–2997
- An F, Zhang X, Zhu Z, Ji Y, He W, Jiang Z, Li M, Guo H** (2012) Coordinated regulation of apical hook development by gibberellins and ethylene in etiolated Arabidopsis seedlings. *Cell Res* **22**: 915–927
- Bäckström S, Elfving N, Nilsson R, Wingsle G, Björklund S** (2007) Purification of a plant mediator from *Arabidopsis thaliana* identifies PFT1 as the Med25 subunit. *Mol Cell* **26**: 717–729
- Bednarek P** (2012) Sulfur-containing secondary metabolites from *Arabidopsis thaliana* and other Brassicaceae with function in plant immunity. *Chembiochem* **13**: 1846–1859
- Berrocal-Lobo M, Molina A, Solano R** (2002) Constitutive expression of *ETHYLENE-RESPONSE-FACTOR1* in Arabidopsis confers resistance to several necrotrophic fungi. *Plant J* **29**: 23–32
- Birkenbihl RP, Diezel C, Somssich IE** (2012) Arabidopsis WRKY33 is a key transcriptional regulator of hormonal and metabolic responses toward *Botrytis cinerea* infection. *Plant Physiol* **159**: 266–285
- Bostock RM** (2005) Signal crosstalk and induced resistance: straddling the line between cost and benefit. *Annu Rev Phytopathol* **43**: 545–580
- Brodersen P, Petersen M, Bjorn Nielsen H, Zhu S, Newman MA, Shokat KM, Rietz S, Parker J, Mundy J** (2006) Arabidopsis MAP kinase 4 regulates salicylic acid- and jasmonic acid/ethylene-dependent responses via EDS1 and PAD4. *Plant J* **47**: 532–546
- Broekaert WF, Terras FRG, Cammue BPA, Vanderleyden J** (1990) An automated quantitative assay for fungal growth-inhibition. *FEMS Microbiol Lett* **69**: 55–59
- Broekgaarden C, Caarls L, Vos IA, Pieterse CM, Van Wees SC** (2015) Ethylene: Traffic controller on hormonal crossroads to defense. *Plant Physiol* **169**: 2371–2379
- Brown RL, Kazan K, McGrath KC, Maclean DJ, Manners JM** (2003) A role for the GCC-box in jasmonate-mediated activation of the *PDF1.2* gene of Arabidopsis. *Plant Physiol* **132**: 1020–1032
- Burch-Smith TM, Schiff M, Liu Y, Dinesh-Kumar SP** (2006) Efficient virus-induced gene silencing in Arabidopsis. *Plant Physiol* **142**: 21–27
- Çevik V, Kidd BN, Zhang P, Hill C, Kiddle S, Denby KJ, Holub EB, Cahill DM, Manners JM, Schenk PM** (2012) MEDIATOR25 acts as an integrative hub for the regulation of jasmonate-responsive gene expression in Arabidopsis. *Plant Physiol* **160**: 541–555
- Chang KN, Zhong S, Weirauch MT, Hon G, Pelizzola M, Li H, Huang SS, Schmitz RJ, Urich MA, Kuo D, et al.** (2013) Temporal transcriptional response to ethylene gas drives growth hormone cross-regulation in Arabidopsis. *Elife* **2**: e00675
- Chao Q, Rothenberg M, Solano R, Roman G, Terzaghi W, Ecker JR** (1997) Activation of the ethylene gas response pathway in Arabidopsis by the nuclear protein ETHYLENE-INSENSITIVE3 and related proteins. *Cell* **89**: 1133–1144
- Cheng MC, Liao PM, Kuo WW, Lin TP** (2013) The Arabidopsis ETHYLENE RESPONSE FACTOR1 regulates abiotic stress-responsive gene expression by binding to different cis-acting elements in response to different stress signals. *Plant Physiol* **162**: 1566–1582
- Cheng Z, Sun L, Qi T, Zhang B, Peng W, Liu Y, Xie D** (2011) The bHLH transcription factor MYC3 interacts with the jasmonate ZIM-domain proteins to mediate jasmonate response in Arabidopsis. *Mol Plant* **4**: 279–288
- Cheong YH, Moon BC, Kim JK, Kim CY, Kim MC, Kim IH, Park CY, Kim JC, Park BO, Koo SC, et al.** (2003) BWMK1, a rice mitogen-activated protein kinase, locates in the nucleus and mediates pathogenesis-related gene expression by activation of a transcription factor. *Plant Physiol* **132**: 1961–1972

- Chini A, Fonseca S, Fernandez G, Adie B, Chico JM, Lorenzo O, Garcia-Casado G, Lopez-Vidriero I, Lozano FM, Ponce MR, et al.** (2007) The JAZ family of repressors is the missing link in jasmonate signalling. *Nature* **448**: 666–671
- Cho YH, Yoo SD** (2011) Signaling role of fructose mediated by FINS1/FBP in *Arabidopsis thaliana*. *PLoS Genet* **7**: e1001263
- Clough SJ, Bent AF** (1998) Floral dip: a simplified method for *Agrobacterium*-mediated transformation of *Arabidopsis thaliana*. *Plant J* **16**: 735–743
- De Boer K, Tillemans S, Pauwels L, Vanden Bossche R, De Sutter V, Vanderhaeghen R, Hilson P, Hamill JD, Goossens A** (2011) APETALA2/ETHYLENE RESPONSE FACTOR and basic helix-loop-helix tobacco transcription factors cooperatively mediate jasmonate-elicited nicotine biosynthesis. *Plant J* **66**: 1053–1065
- De Vos M, Van Oosten VR, Van Poecke RM, Van Pelt JA, Pozo MJ, Mueller MJ, Buchala AJ, Mettraux JP, Van Loon LC, Dicke M, et al.** (2005) Signal signature and transcriptome changes of *Arabidopsis* during pathogen and insect attack. *Mol Plant Microbe Interact* **18**: 923–937
- Dong X** (1998) SA, JA, ethylene, and disease resistance in plants. *Curr Opin Plant Biol* **1**: 316–323
- Eichmann R, Schafer P** (2012) The endoplasmic reticulum in plant immunity and cell death. *Front Plant Sci* **3**: 200
- Fernandez-Calvo P, Chini A, Fernandez-Barbero G, Chico JM, Gimenez-Ibanez S, Geerinck J, Eeckhout D, Schweizer F, Godoy M, Franco-Zorrilla JM, et al.** (2011) The *Arabidopsis* bHLH transcription factors MYC3 and MYC4 are targets of JAZ repressors and act additively with MYC2 in the activation of jasmonate responses. *Plant Cell* **23**: 701–715
- Feys BJ, Parker JE** (2000) Interplay of signaling pathways in plant disease resistance. *Trends Genet* **16**: 449–455
- Glazebrook J** (2005) Contrasting mechanisms of defense against biotrophic and necrotrophic pathogens. *Annu Rev Phytopathol* **43**: 205–227
- Gosti F, Bertauche N, Vartanian N, Giraudat J** (1995) Abscisic acid-dependent and -independent regulation of gene expression by progressive drought in *Arabidopsis thaliana*. *Mol Gen Genet* **246**: 10–18
- Gu YQ, Yang C, Thara VK, Zhou J, Martin GB** (2000) *Pti4* is induced by ethylene and salicylic acid, and its product is phosphorylated by the Pto kinase. *Plant Cell* **12**: 771–785
- Guo H, Ecker JR** (2003) Plant responses to ethylene gas are mediated by SCFEBF1/EBF2-dependent proteolysis of EIN3 transcription factor. *Cell* **115**: 667–677
- Hao D, Ohme-Takagi M, Sarai A** (1998) Unique mode of GCC box recognition by the DNA-binding domain of ethylene-responsive element-binding factor (ERF domain) in plant. *J Biol Chem* **273**: 26857–26861
- He X, Jiang J, Wang CQ, Dehesh K** (2017) ORA59 and EIN3 interaction couples jasmonate-ethylene synergistic action to antagonistic salicylic acid regulation of *PDF* expression. *J Integr Plant Biol* **59**: 275–287
- Hickman R, Van Verk MC, Van Dijken AJH, Mendes MP, Vroegop-Vos IA, Caarls L, Steenbergen M, Van der Nagel I, Wesselink GJ, Jironkin A, et al.** (2017) Architecture and dynamics of the jasmonic acid gene regulatory network. *Plant Cell* **29**: 2086–2105
- Huang PX, Dong Z, Guo PR, Zhang X, Qiu YP, Li BS, Wang YC, Guo HW** (2020) Salicylic acid suppresses apical hook formation via NPR1-mediated repression of EIN3 and EIL1 in *Arabidopsis*. *Plant Cell* **32**: 612–629
- Huang PY, Catinot J, Zimmerli L** (2016) Ethylene response factors in *Arabidopsis* immunity. *J Exp Bot* **67**: 1231–1241
- Itzhaki H, Maxson JM, Woodson WR** (1994) An ethylene-responsive enhancer element is involved in the senescence-related expression of the carnation glutathione-S-transferase (*GST1*) gene. *Proc Natl Acad Sci USA* **91**: 8925–8929
- Jefferson RA, Kavanagh TA, Bevan MW** (1987) GUS fusions: beta-glucuronidase as a sensitive and versatile gene fusion marker in higher plants. *EMBO J* **6**: 3901–3907
- Joo S, Kim WT** (2007) A gaseous plant hormone ethylene: The signaling pathway. *J Plant Biol* **50**: 109–116
- Ju C, Yoon GM, Shemansky JM, Lin DY, Ying ZI, Chang J, Garrett WM, Kessenbrock M, Groth G, Tucker ML, et al.** (2012) CTR1 phosphorylates the central regulator EIN2 to control ethylene hormone signaling from the ER membrane to the nucleus in *Arabidopsis*. *Proc Natl Acad Sci USA* **109**: 19486–19491
- Kagaya Y, Ohmiya K, Hattori T** (1999) RAV1, a novel DNA-binding protein, binds to bipartite recognition sequence through two distinct DNA-binding domains uniquely found in higher plants. *Nucleic Acids Res* **27**: 470–478
- Katsir L, Schillmiller AL, Staswick PE, He SY, Howe GA** (2008) COI1 is a critical component of a receptor for jasmonate and the bacterial virulence factor coronatine. *Proc Natl Acad Sci USA* **105**: 7100–7105
- Kieber JJ, Rothenberg M, Roman G, Feldmann KA, Ecker JR** (1993) CTR1, a negative regulator of the ethylene response pathway in *Arabidopsis*, encodes a member of the raf family of protein kinases. *Cell* **72**: 427–441
- Kim D, Paggi JM, Park C, Bennett C, Salzberg SL** (2019) Graph-based genome alignment and genotyping with HISAT2 and HISAT-genotype. *Nat Biotechnol* **37**: 907–915
- Kim HG, Kwon SJ, Jang YJ, Chung JH, Nam MH, Park OK** (2014) GDSL lipase 1 regulates ethylene signaling and ethylene-associated systemic immunity in *Arabidopsis*. *FEBS Lett* **588**: 1652–1658
- Kim HG, Kwon SJ, Jang YJ, Nam MH, Chung JH, Na YC, Guo H, Park OK** (2013) GDSL LIPASE1 modulates plant immunity through feedback regulation of ethylene signaling. *Plant Physiol* **163**: 1776–1791
- Konishi M, Yanagisawa S** (2008) Ethylene signaling in *Arabidopsis* involves feedback regulation via the elaborate control of *EBF2* expression by EIN3. *Plant J* **55**: 821–831
- Koornneef A, Pieterse CM** (2008) Cross talk in defense signaling. *Plant Physiol* **146**: 839–844
- Kunkel BN, Brooks DM** (2002) Cross talk between signaling pathways in pathogen defense. *Curr Opin Plant Biol* **5**: 325–331
- Kwon SJ, Jin HC, Lee S, Nam MH, Chung JH, Kwon SI, Ryu CM, Park OK** (2009) GDSL lipase-like 1 regulates systemic resistance associated with ethylene signaling in *Arabidopsis*. *Plant J* **58**: 235–245
- Laluk K, Mengiste T** (2011) The *Arabidopsis* extracellular UNUSUAL SERINE PROTEASE INHIBITOR functions in resistance to necrotrophic fungi and insect herbivory. *Plant J* **68**: 480–494
- Lee DS, Kim YC, Kwon SJ, Ryu CM, Park OK** (2017) The *Arabidopsis* cysteine-rich receptor-like kinase CRK36 regulates immunity through interaction with the cytoplasmic kinase BIK1. *Front Plant Sci* **8**: 1856
- Lee MH, Jeon HS, Kim HG, Park OK** (2017) An *Arabidopsis* NAC transcription factor NAC4 promotes pathogen-induced cell death under negative regulation by microRNA164. *New Phytol* **214**: 343–360
- Li W, Ma M, Feng Y, Li H, Wang Y, Ma Y, Li M, An F, Guo H** (2015) EIN2-directed translational regulation of ethylene signaling in *Arabidopsis*. *Cell* **163**: 670–683
- Li Z, Peng J, Wen X, Guo H** (2013) Ethylene-insensitive3 is a senescence-associated gene that accelerates age-dependent leaf senescence by directly repressing *miR164* transcription in *Arabidopsis*. *Plant Cell* **25**: 3311–3328
- Licausi F, Ohme-Takagi M, Perata P** (2013) APETALA2/ethylene responsive factor (AP2/ERF) transcription factors: mediators of stress responses and developmental programs. *New Phytol* **199**: 639–649
- Lorenzo O, Piqueras R, Sanchez-Serrano JJ, Solano R** (2003) ETHYLENE RESPONSE FACTOR1 integrates signals from ethylene and jasmonate pathways in plant defense. *Plant Cell* **15**: 165–178

- Lou YR, Bor M, Yan J, Preuss AS, Jander G (2016) Arabidopsis NATA1 acetylates putrescine and decreases defense-related hydrogen peroxide accumulation. *Plant Physiol* **171**: 1443–1455
- Love MI, Huber W, Anders S (2014) Moderated estimation of fold change and dispersion for RNA-seq data with DESeq2. *Genome Biol* **15**: 550
- Meng X, Xu J, He Y, Yang KY, Mordorski B, Liu Y, Zhang S (2013) Phosphorylation of an ERF transcription factor by Arabidopsis MPK3/MPK6 regulates plant defense gene induction and fungal resistance. *Plant Cell* **25**: 1126–1142
- Montgomery J, Goldman S, Deikman J, Margossian L, Fischer RL (1993) Identification of an ethylene-responsive region in the promoter of a fruit ripening gene. *Proc Natl Acad Sci USA* **90**: 5939–5943
- Morikawa-Ichinose T, Miura D, Zhang L, Kim SJ, Maruyama-Nakashita A (2020) Involvement of BGLU30 in glucosinolate catabolism in the Arabidopsis leaf under dark conditions. *Plant Cell Physiol* **61**: 1095–1106
- Mulema JM, Denby KJ (2012) Spatial and temporal transcriptomic analysis of the *Arabidopsis thaliana*-*Botrytis cinerea* interaction. *Mol Biol Rep* **39**: 4039–4049
- Niu Y, Figueroa P, Browse J (2011) Characterization of JAZ-interacting bHLH transcription factors that regulate jasmonate responses in Arabidopsis. *J Exp Bot* **62**: 2143–2154
- Oh IS, Park AR, Bae MS, Kwon SJ, Kim YS, Lee JE, Kang NY, Lee S, Cheong H, Park OK (2005) Secretome analysis reveals an Arabidopsis lipase involved in defense against *Alternaria brassicicola*. *Plant Cell* **17**: 2832–2847
- Ohme-Takagi M, Shinshi H (1995) Ethylene-inducible DNA binding proteins that interact with an ethylene-responsive element. *Plant Cell* **7**: 173–182
- Ou B, Yin KQ, Liu SN, Yang Y, Gu T, Wing Hui JM, Zhang L, Miao J, Kondou Y, Matsui M, et al. (2011) A high-throughput screening system for Arabidopsis transcription factors and its application to Med25-dependent transcriptional regulation. *Mol Plant* **4**: 546–555
- Penninckx IA, Thomma BP, Buchala A, Metraux JP, Broekaert WF (1998) Concomitant activation of jasmonate and ethylene response pathways is required for induction of a plant defensin gene in Arabidopsis. *Plant Cell* **10**: 2103–2113
- Pertea M, Pertea GM, Antonescu CM, Chang TC, Mendell JT, Salzberg SL (2015) StringTie enables improved reconstruction of a transcriptome from RNA-seq reads. *Nat Biotechnol* **33**: 290–295
- Pfalz M, Mikkelsen MD, Bednarek P, Olsen CE, Halkier BA, Kroymann J (2011) Metabolic engineering in *Nicotiana benthamiana* reveals key enzyme functions in Arabidopsis indole glucosinolate modification. *Plant Cell* **23**: 716–729
- Phukan UJ, Jeena GS, Tripathi V, Shukla RK (2017) Regulation of Apetala2/ethylene response factors in plants. *Front Plant Sci* **8**: 150
- Pieterse CM, Leon-Reyes A, Van der Ent S, Van Wees SC (2009) Networking by small-molecule hormones in plant immunity. *Nat Chem Biol* **5**: 308–316
- Pieterse CM, Van der Does D, Zamioudis C, Leon-Reyes A, Van Wees SC (2012) Hormonal modulation of plant immunity. *Annu Rev Cell Dev Biol* **28**: 489–521
- Pogorelko GV, Mokryakova M, Fursova OV, Abdeeva I, Piruzian ES, Bruskin SA (2014) Characterization of three *Arabidopsis thaliana* immunophilin genes involved in the plant defense response against *Pseudomonas syringae*. *Gene* **538**: 12–22
- Potuschak T, Lechner E, Parmentier Y, Yanagisawa S, Grava S, Koncz C, Genschik P (2003) EIN3-dependent regulation of plant ethylene hormone signaling by two Arabidopsis F box proteins: EBF1 and EBF2. *Cell* **115**: 679–689
- Pre M, Atallah M, Champion A, De Vos M, Pieterse CM, Memelink J (2008) The AP2/ERF domain transcription factor ORA59 integrates jasmonic acid and ethylene signals in plant defense. *Plant Physiol* **147**: 1347–1357
- Qiao H, Shen Z, Huang SS, Schmitz RJ, Urlich MA, Briggs SP, Ecker JR (2012) Processing and subcellular trafficking of ER-tethered EIN2 control response to ethylene gas. *Science* **338**: 390–393
- Reyes F, Marchant L, Norambuena L, Nilo R, Silva H, Orellana A (2006) AtUTr1, a UDP-glucose/UDP-galactose transporter from *Arabidopsis thaliana*, is located in the endoplasmic reticulum and up-regulated by the unfolded protein response. *J Biol Chem* **281**: 9145–9151
- Ritchie ME, Phipson B, Wu D, Hu Y, Law CW, Shi W, Smyth GK (2015) limma powers differential expression analyses for RNA-sequencing and microarray studies. *Nucleic Acids Res* **43**: e47
- Roman G, Ecker JR (1995) Genetic analysis of a seedling stress response to ethylene in Arabidopsis. *Philos Trans R Soc Lond B Biol Sci* **350**: 75–81
- Schenk PM, Kazan K, Wilson I, Anderson JP, Richmond T, Somerville SC, Manners JM (2000) Coordinated plant defense responses in Arabidopsis revealed by microarray analysis. *Proc Natl Acad Sci USA* **97**: 11655–11660
- Sheard LB, Tan X, Mao H, Withers J, Ben-Nissan G, Hinds TR, Kobayashi Y, Hsu FF, Sharon M, Browse J, et al. (2010) Jasmonate perception by inositol-phosphate-potentiated COI1-JAZ co-receptor. *Nature* **468**: 400–405
- Solano L, Stepanova A, Chao Q, Ecker JR (1998) Nuclear events in ethylene signaling: a transcriptional cascade mediated by ETHYLENE-INSENSITIVE3 and ETHYLENE-RESPONSE-FACTOR1. *Genes Dev* **12**: 3703–3714
- Spoel SH, Dong X (2008) Making sense of hormone crosstalk during plant immune responses. *Cell Host Microbe* **3**: 348–351
- Thines B, Katsir L, Melotto M, Niu Y, Mandaokar A, Liu G, Nomura K, He SY, Howe GA, Browse J (2007) JAZ repressor proteins are targets of the SCF(COI1) complex during jasmonate signalling. *Nature* **448**: 661–665
- Thomma BP, Eggermont K, Penninckx IA, Mauch-Mani B, Vogelsang R, Cammue BP, Broekaert WF (1998) Separate jasmonate-dependent and salicylate-dependent defense-response pathways in Arabidopsis are essential for resistance to distinct microbial pathogens. *Proc Natl Acad Sci USA* **95**: 15107–15111
- Thomma BP, Eggermont K, Tierens KF, Broekaert WF (1999) Requirement of functional *ethylene-insensitive 2* gene for efficient resistance of Arabidopsis to infection by *Botrytis cinerea*. *Plant Physiol* **121**: 1093–1102
- Van der Does D, Leon-Reyes A, Koornneef A, Van Verk MC, Rodenburg N, Pauwels L, Goossens A, Korbes AP, Memelink J, Ritsema T, et al. (2013) Salicylic acid suppresses jasmonic acid signaling downstream of SCFCOI1-JAZ by targeting GCC promoter motifs via transcription factor ORA59. *Plant Cell* **25**: 744–761
- Wang P, Du Y, Zhao X, Miao Y, Song CP (2013) The MPK6-ERF6-ROS-responsive cis-acting Element7/GCC box complex modulates oxidative gene transcription and the oxidative response in Arabidopsis. *Plant Physiol* **161**: 1392–1408
- Welchen E, Viola IL, Kim HJ, Prendes LP, Comelli RN, Hong JC, Gonzalez DH (2009) A segment containing a G-box and an ACGT motif confers differential expression characteristics and responses to the Arabidopsis *Cytc-2* gene, encoding an isoform of cytochrome c. *J Exp Bot* **60**: 829–845
- Wen X, Zhang C, Ji Y, Zhao Q, He W, An F, Jiang L, Guo H (2012) Activation of ethylene signaling is mediated by nuclear translocation of the cleaved EIN2 carboxyl terminus. *Cell Res* **22**: 1613–1616
- Windram O, Madhou P, McHattie S, Hill C, Hickman R, Cooke E, Jenkins DJ, Penfold CA, Baxter L, Breeze E, et al. (2012) Arabidopsis defense against *Botrytis cinerea*: chronology and regulation deciphered by high-resolution temporal transcriptomic analysis. *Plant Cell* **24**: 3530–3557
- Yan J, Zhang C, Gu M, Bai Z, Zhang W, Qi T, Cheng Z, Peng W, Luo H, Nan F, Wang Z, Xie D (2009) The Arabidopsis CORONATINE INSENSITIVE1 protein is a jasmonate receptor. *Plant Cell* **21**: 2220–2236
- Yang Y, Ou B, Zhang J, Si W, Gu H, Qin G, Qu LJ (2014) The Arabidopsis Mediator subunit MED16 regulates iron homeostasis

- by associating with EIN3/EIL1 through subunit MED25. *Plant J* **77**: 838–851
- Yang YX, Ahammed GJ, Wu C, Fan SY, Zhou YH** (2015) Crosstalk among jasmonate, salicylate and ethylene signaling pathways in plant disease and immune responses. *Curr Protein Pept Sci* **16**: 450–461
- Yoo SD, Cho YH, Sheen J** (2007) Arabidopsis mesophyll protoplasts: a versatile cell system for transient gene expression analysis. *Nat Protoc* **2**: 1565–1572
- Zander M, Chen S, Imkampe J, Thurow C, Gatz C** (2012) Repression of the *Arabidopsis thaliana* jasmonic acid/ethylene-induced defense pathway by TGA-interacting glutaredoxins depends on their C-terminal ALWL motif. *Mol Plant* **5**: 831–840
- Zander M, Thurow C, Gatz C** (2014) TGA transcription factors activate the salicylic acid-suppressible branch of the ethylene-induced defense program by regulating *ORA59* expression. *Plant Physiol* **165**: 1671–1683
- Zarei A, Korbes AP, Younessi P, Montiel G, Champion A, Memelink J** (2011) Two GCC boxes and AP2/ERF-domain transcription factor *ORA59* in jasmonate/ethylene-mediated activation of the *PDF1.2* promoter in Arabidopsis. *Plant Mol Biol* **75**: 321–331
- Zhang L, Kawaguchi R, Morikawa-Ichinose T, Allahham A, Kim SJ, Maruyama-Nakashita A** (2020) Sulfur deficiency-induced glucosinolate catabolism attributed to two beta-glucosidases, BGLU28 and BGLU30, is required for plant growth maintenance under sulfur deficiency. *Plant Cell Physiol* **61**: 803–813
- Zhong S, Zhao M, Shi T, Shi H, An F, Zhao Q, Guo H** (2009) EIN3/EIL1 cooperate with PIF1 to prevent photo-oxidation and to promote greening of Arabidopsis seedlings. *Proc Natl Acad Sci USA* **106**: 21431–21436
- Zhu Z** (2014) Molecular basis for jasmonate and ethylene signal interactions in Arabidopsis. *J Exp Bot* **65**: 5743–5748
- Zhu Z, An F, Feng Y, Li P, Xue L, A M, Jiang Z, Kim JM, To TK, Li W, et al.** (2011) Derepression of ethylene-stabilized transcription factors (EIN3/EIL1) mediates jasmonate and ethylene signaling synergy in Arabidopsis. *Proc Natl Acad Sci USA* **108**: 12539–12544
- Zhu Z, Lee B** (2015) Friends or foes: new insights in jasmonate and ethylene co-actions. *Plant Cell Physiol* **56**: 414–420